State of the Practice and Art for Structural Health Monitoring of Bridge Substructures

U.S. Department of Transportation
Federal Highway Administration

FOREWORD

This project was originally intended to show the merits of substructure health monitoring via a review of the few well-documented cases wherein a concerted effort to assess the long-term performance of foundations were in place. While these efforts were underway, the St. Anthony Falls Bridge, also known as the I-35W bridge, over the Mississippi River in Minneapolis, MN, collapsed in August 2007 in the middle of rush hour, killing 13 people. This incident revealed to engineers the United States' failing infrastructure. As a result, the project was redirected to aid the Minnesota Department of Transportation and the Federal Highway Administration in providing an effective yet economical means to monitor the new substructure during construction and in future years. That which was intended to be a review of previously performed and available technologies became a demonstration of available technologies and how they play into the role of foundation health monitoring.

This final report provides an overview of the benefits of remote data acquisitions systems for both short- and long-term monitoring of highway bridges. It contains background information and presents capabilities of data collection systems for highway bridges and concludes with an evaluation of a recent case study where remote health monitoring was successfully implemented. Interested audiences of the report include bridge engineers, highway officials, and municipality officials.

Jorge E. Pagán-Ortiz
Director, Office of Infrastructure
Research and Development

TECHNICAL DOCUMENTATION PAGE

1. Report No. FHWA-HRT-09-040	2. Government Accession No.	3. Recipient's Catalog No.	
4. Title and Subtitle State of the Practice and Art for Structural Health Monitoring of Bridge Substructures		5. Report Date May 2014	
		6. Performing Organization Code	
7. Author(s) J. Collins, G. Mullins, C. Lewis, and D. Winters		8. Performing Organization Report No. G07-M-279	
9. Performing Organization Name and Address Foundation and Geotechnical Engineering, LLC 712 East Alsobrook Street, Suite 3 Plant City, FL 33563 Under contract from: Engineering and Software Consultants, Inc. 14123 Robert Paris Court Chantilly, VA 20151		10. Work Unit No. (TRAIS)	
		11. Contract or Grant No. DTFH61-07-00033	
12. Sponsoring Agency Name and Address Office of Infrastructure Federal Highway Administration 6300 Georgetown Pike McLean, VA 22101-2296		13. Type of Report and Period Covered Final Report	
		14. Sponsoring Agency Code	
15. Supplementary Notes The project began under the supervision of Carl Ealy (FHWA retired) and concluded under the supervision Mike Adams (FHWA, Turner-Fairbank Highway Research Center).			
16. Abstract In an age of technological advances, the ability to monitor the performance of bridge foundations has evolved such that both short- and long-term data acquisition of embedded gauges is not only available but also cost effective. Case studies were documented that show the merits of using embedded gauges and low-cost data collection systems to provide increased quality assurance during construction as well as a means to monitor the health of the foundations while in service.			
17. Key Words Data acquisition, Remote health monitoring, Embedded instrumentation, Bridge foundations		18. Distribution Statement No restrictions.	
19. Security Classif. (of this report) Unclassified	20. Security Classif. (of this page) Unclassified	21. No. of Pages 97	22. Price

Form DOT F 1700.7 (8-72)   Reproduction of completed page authorized

SI* (MODERN METRIC) CONVERSION FACTORS

APPROXIMATE CONVERSIONS TO SI UNITS

Symbol	When You Know	Multiply By	To Find	Symbol
LENGTH				
in	inches	25.4	millimeters	mm
ft	feet	0.305	meters	m
yd	yards	0.914	meters	m
mi	miles	1.61	kilometers	km
AREA				
in^2	square inches	645.2	square millimeters	mm^2
ft^2	square feet	0.093	square meters	m^2
yd^2	square yard	0.836	square meters	m^2
ac	acres	0.405	hectares	ha
mi^2	square miles	2.59	square kilometers	km^2
VOLUME				
fl oz	fluid ounces	29.57	milliliters	mL
gal	gallons	3.785	liters	L
ft^3	cubic feet	0.028	cubic meters	m^3
yd^3	cubic yards	0.765	cubic meters	m^3
NOTE: volumes greater than 1000 L shall be shown in m^3				
MASS				
oz	ounces	28.35	grams	g
lb	pounds	0.454	kilograms	kg
T	short tons (2000 lb)	0.907	megagrams (or "metric ton")	Mg (or "t")
TEMPERATURE (exact degrees)				
^oF	Fahrenheit	5 (F-32)/9 or (F-32)/1.8	Celsius	^oC
ILLUMINATION				
fc	foot-candles	10.76	lux	lx
fl	foot-Lamberts	3.426	candela/m^2	cd/m^2
FORCE and PRESSURE or STRESS				
lbf	poundforce	4.45	newtons	N
lbf/in^2	poundforce per square inch	6.89	kilopascals	kPa

APPROXIMATE CONVERSIONS FROM SI UNITS

Symbol	When You Know	Multiply By	To Find	Symbol
LENGTH				
mm	millimeters	0.039	inches	in
m	meters	3.28	feet	ft
m	meters	1.09	yards	yd
km	kilometers	0.621	miles	mi
AREA				
mm^2	square millimeters	0.0016	square inches	in^2
m^2	square meters	10.764	square feet	ft^2
m^2	square meters	1.195	square yards	yd^2
ha	hectares	2.47	acres	ac
km^2	square kilometers	0.386	square miles	mi^2
VOLUME				
mL	milliliters	0.034	fluid ounces	fl oz
L	liters	0.264	gallons	gal
m^3	cubic meters	35.314	cubic feet	ft^3
m^3	cubic meters	1.307	cubic yards	yd^3
MASS				
g	grams	0.035	ounces	oz
kg	kilograms	2.202	pounds	lb
Mg (or "t")	megagrams (or "metric ton")	1.103	short tons (2000 lb)	T
TEMPERATURE (exact degrees)				
^oC	Celsius	1.8C+32	Fahrenheit	^oF
ILLUMINATION				
lx	lux	0.0929	foot-candles	fc
cd/m^2	candela/m^2	0.2919	foot-Lamberts	fl
FORCE and PRESSURE or STRESS				
N	newtons	0.225	poundforce	lbf
kPa	kilopascals	0.145	poundforce per square inch	lbf/in^2

*SI is the symbol for the International System of Units. Appropriate rounding should be made to comply with Section 4 of ASTM E380.
(Revised March 2003)

TABLE OF CONTENTS

LIST OF FIGURES

LIST OF TABLES

CHAPTER 1. INTRODUCTION

In order to develop safe, cost-effective, and reliable structures in the future, it is imperative for designers to cross-check assumptions made during the design phase with the conditions that the structure will actually experience. Ideally, the designer's understanding of those conditions is reflected in the design, and the structure's response to such loads should show close agreement. However, in many cases, the worst-case scenarios controlling the design do not actually occur; therefore, the true structural design is never fully verified. This does not suggest that the design is unreasonable; rather, it indicates that the response to extreme loads remains somewhat hypothetical. In the instances where extreme events occur, there are rarely quantifiable measures of how the structure performed due to the absence of permanently installed or embedded instrumentation along with a continuously sampling acquisition methodology. More common and less critical loading states can and have been used to provide insight into the response that can be either extrapolated or used to provide a lesser degree of verification. However, this type of post-construction verification is not commonplace.

Civil engineering applications are typically the last to adopt and/or receive the inroads into newer technological breakthroughs that are used in other arenas of science. Similar to the personal computer industry, advances in wireless microwave and satellite communications occur daily. Even some past technologies have not been fully implemented or explored with the exception of atypical high profile structures (i.e., in high-risk seismic regions). The upshot is that many past technologies are now relatively inexpensive and can be reasonably applied to civil-type structures more routinely.

As a civil engineering application, remote monitoring has only begun to make a breakthrough into the field, having historically been used as a research and development tool. Its benefits are finally coming to realization. There is a push for the United States to become wireless; therefore, it has increasingly become a necessity for civil engineering to lead the way, specifically in the area of remote structural health monitoring (SHM).

Remote monitoring, at its most basic, provides users with a way to collect data from an event, such as a foundation capacity test or ongoing thermal recording, and then transmit the collected data to another location, such as a database or spreadsheet file on a computer. This concept can be taken one step further by introducing limits on the data collector for alerting users or programming triggers on the data collector to initiate retroactive data collection and transmitting.

Remote monitoring can be used for many different civil engineering applications, from quality assurance in construction to ongoing health verification. It can provide assurance to engineers and society as a whole that infrastructure withstands into the next generation. Furthermore, as new technology is upgraded, the cost and effectiveness benefits of remote monitoring continue to increase. As with all new approaches, they are not fully embraced by the construction and engineering society alike until there are recognizable savings. However, with catastrophic failures like the St. Anthony Falls Bridge (also referred to as the I-35W bridge) collapse over the Mississippi River, additional pressure to investigate the use and/or require the implementation of new technological advances plays into acceptance.

PROBLEM STATEMENT

As a civil engineering tool, remote monitoring is a priceless benefit for the health monitoring of structural members. Currently, the most common monitoring technique for inspecting bridges is visual inspection. Based on standards set by the Florida Department of Transportation and the Federal Highway Administration (FHWA), every bridge is required to undergo a visual inspection once every 2 years. While this method is satisfactory for structurally sufficient noncritical structures, it does not provide a reliable way to determine the actual health of a structure. Providing a remote monitoring system will allow researchers to monitor a bridge in real time at a remote location. This method will help reduce man hours and provide accurate results and up-to-date data to assess the structural integrity of a structure and not just its visual appearance. Foundations, however, are not readily amenable to retrofitted instrumentation regardless of whether or not remote monitoring is employed. Therefore, a concerted effort to incorporate these more peripheral options must be considered at the design phase for proper inclusion during construction.

SCOPE AND SIGNIFICANCE

This study provides a brief overview of previous foundation health monitoring schemes. It also proposes the use of wireless communication and Internet systems technologies as a means of providing remote monitoring capabilities for structural members or systems for agencies such as State transportation departments and FHWA. However, the use of these technologies as described is not limited to the use by these agencies. The original intent of the research was not to determine the best technology to carry out the project but rather to provide examples of monitoring procedures and data from a variety of tests that were monitored using this concept.

Another focus of this study is to provide several different monitoring techniques that can be applied to a structural member to enable it to be monitored throughout its life. These techniques include sensors and devices that would provide data related to temperature, load, strain, and video recording. All of these parameters are vital for the determination of the structural health of a member or system.

REPORT ORGANIZATION

This report consists of five chapters. Chapter 1 introduces the topic of the report. Chapter 2 summarizes the state of SHM in general with an emphasis on substructure health monitoring (SSHM) and the ability to convert current wired systems into wireless. Chapter 3 provides an in-depth look at a case study that was carried out on an innovative type of drilled shaft. It is used to highlight the convenience and, in some instances, limitations and considerations that should be addressed when planning a prototypical remote monitoring program. Therein, it summarizes the successes and learning experiences gained from this project. Chapter 4 discusses the culmination of all the work performed on this project and reviews the short- and long-term monitoring procedures implemented on the I-35W bridge. It also explains the construction, setup, instrumentation, monitoring procedure, and results for a full-scale remote SHM system. Chapter 5 summarizes the main discoveries made throughout the study and presents conclusions and recommendations for future work.

CHAPTER 2. STATE OF THE PRACTICE

From an investigation into the state of the practice of SHM, it is evident that there are a number of different monitoring systems and techniques. All of them have their pros and cons, but each can be useful to a certain degree. Most of the advances in SHM have been made in the monitoring of the superstructure elements of bridges and other structures; however, the importance of SSHM cannot be underestimated.

Since a large amount of the modern SHM technology is already widely used and documented as it pertains to superstructure monitoring, this review of the state of the practice will primarily focus on common technology and its practicality for use in a SSHM system.

GENERAL MONITORING SYSTEMS

Monitoring systems range in their functionality, cost, applied technology, and monitoring approach. A system generally contains three components: (1) a measuring device, (2) a method of reading that device, and (3) a method of storing the measurements. Depending on the complexity of the measurement being taken, the measuring device and readout component may be one and the same, such as dial gauges or pressure gauges (see figure 1).

Figure 1. Photo. Standard rotary dial gauges.

These devices convert a measurement parameter into mechanical gauge movement and can be considered the most basic of transducers as they transfer one physical aspect into another. Virtually all types of measurements have specialized devices to read that particular occurrence (i.e., time, displacement, velocity, acceleration, load, pressure, frequency, electromagnetic field (EMF), light intensity, strain, sound intensity, X-rays, voltage, inductance, capacitance, etc.).

For most measurement types, there are many ways to take those measurements, which in turn, dictate the capabilities and/or limitations of a monitoring system.

The most basic systems use fully manual devices and readouts (e.g., dial gauges, proving rings, pressure gauges, etc.) coupled with manual record keeping. The limitations imposed on this method by requiring physical onsite personnel (i.e., recording/storage rate, man hours, and travel) are in some ways offset by the unforeseen observations and the ability to react to and record unplanned secondary happenings. The most exotic systems use complex measurement devices requiring sophisticated readout units coupled with a multifunctional data acquisition system (DAS) capable of sending the recorded data via cellular or satellite communications. These systems are often enabled to accept remote configuration/scheme changes, are self powered or self contained, and require little to no site visits. The most extreme cases of this type of system would likely be used by the National Aeronautics and Space Administration for space exploration because it is impossible to access the unit during use. Aside from the obvious cost, these systems are rarely adaptable to unforeseen occurrences. For SHM and SSHM applications, some midrange systems can be selected to provide a balance between equipment costs and required onsite man hours, which will allow most projects to be affordable.

CASE STUDY

One sample study performed by FHWA, the Washington State Department of Transportation, the city of Seattle, WA, and the bridge design team on the West Seattle freeway bridge incorporated a SSHM protocol.[1] This study is one of few that focused on substructural elements of a bridge pier during the construction of the bridge, as well as data collection over time. The West Seattle freeway bridge was built between 1981 and 1984. The original bridge was struck by a freighter in 1978 and was deemed inoperable as a result of the incident. The goal was to advance the state of the art of pile group design and analysis, and the information collected would be used in increasing pile group efficiency.

Authorities in Seattle, WA, authorized the use of instrumentation on pier EA-31, which is a single-column pier that supports the eastbound approach ramp from Spokane Street near the East Waterway and the Duwamish River (see figure 2).[1]
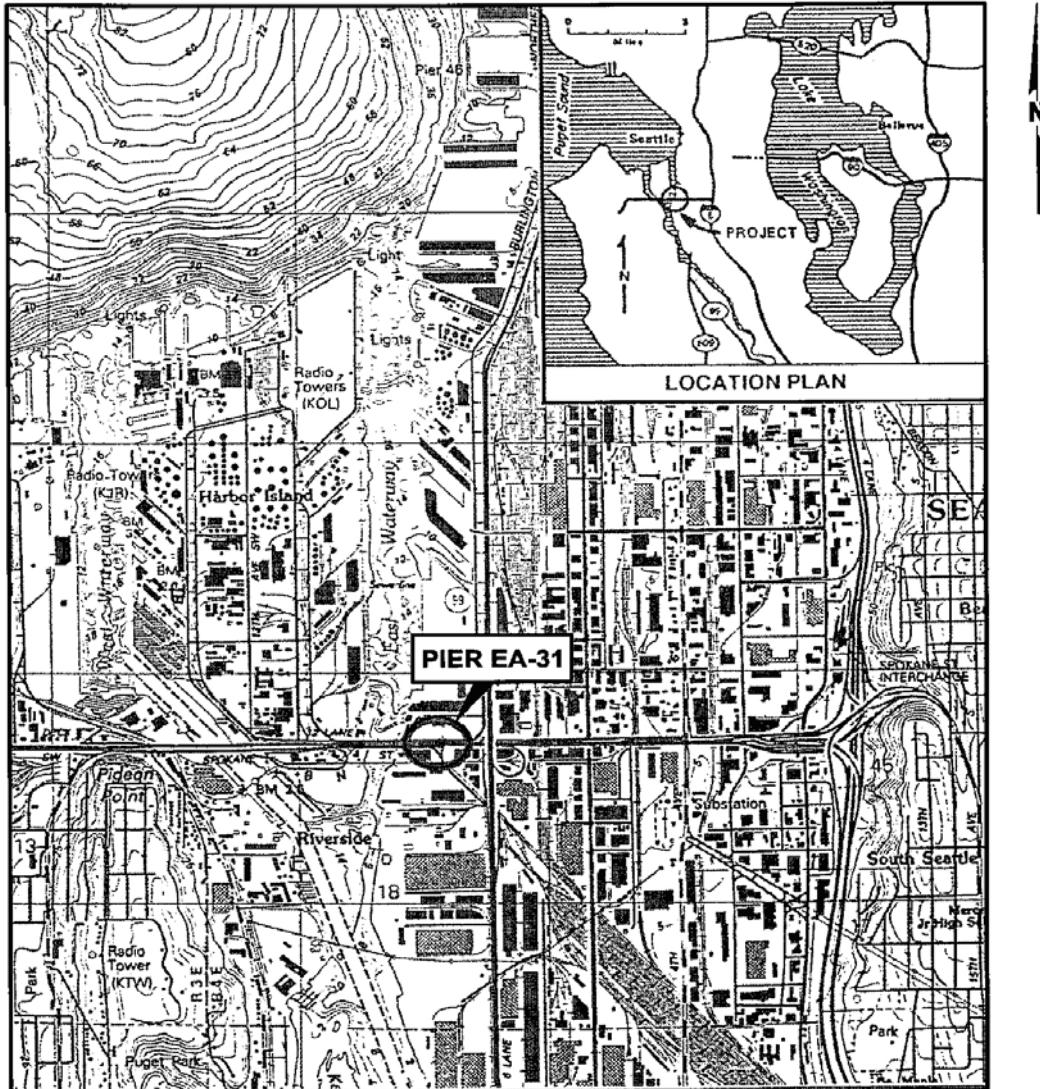
Figure 2. Illustration. Pier EA-31 site map.[1]

As stated previously, the purpose of this project was to improve the state of the art of pile group design and analysis. This was done by collecting information regarding the load distribution among the pile group, the load transfer from the piles to the soil, the portion of the load transferred from the pier footing to the piles, and the settlement of the pier footing. Furthermore, the results gathered from this data were compared with theoretical predictions that would either validate the theoretical models or allow for the modification of those models.

In order to provide measurements for the data collection criteria, measurements were selected by first measuring pile tip load as well as the load at six elevations along the pile to determine the individual pile load distribution. A load cell placed at the pile tip permitted direct measurement of the load. Next, six telltale rods were installed on each pile to determine the pile tip displacement. The pile deformation measured by the rods was converted to strain and used as a check. Strain gauges were then installed at the top of the piles, which provided information about the load transferred from the pier footing to the individual piles. Settlement of the pier footing

5

was then measured by using a precise surveying measurement at the four corners of the footing. Last, soil settlement below the pier footing and within the pile group was measured to determine the soil's reaction to the loading and subsequent deformation of the piles.

In total, 3 of the 12 piles were instrumented with a load cell at the pile tip, along with 6 elevations of strain gauge pairs and a 5-position telltale extensometer (see 1 ft = 0.305 m

figure 3). Data from the instrumentation were collected in the field using portable manual readout units and recorded on field sheets. During construction, the measurements were made at irregular intervals dependent on accessibility and other constraints due to the construction progress. The instruments were monitored as each significant phase of construction was completed to provide realistic data from the construction process. Instrumentation monitoring was conducted throughout construction and continued through 1987, 5 years after the start of construction.[1] Data were again collected in September 1988, September 1989, and October 1993. Two additional sets of data were taken in 1999 and 2002, which extended the period of monitoring to 20 years. The report presents a summary of the existing working gauges as well as the date at which failed gauges no longer worked (see table 1).[1]

40 ft

30 ft

20 ft — CAP BEAM

10 ft — 17'

PIER FOOTING — 8'

EL +3

EL −5 — Gage 6 EL −6

−10 ft

−20 ft — Gage 5 EL −22

24'

−30 ft

−40 ft — 14' — Gage 4 EL −38

PLAN VIEW

−50 ft — Gage 3 EL −55

−60 ft

−70 ft — PRESTRESSED CONCRETE PILES

−80 ft — Gage 2 EL −73

−90 ft — Gage 1 EL −90

−100 ft — EL −97
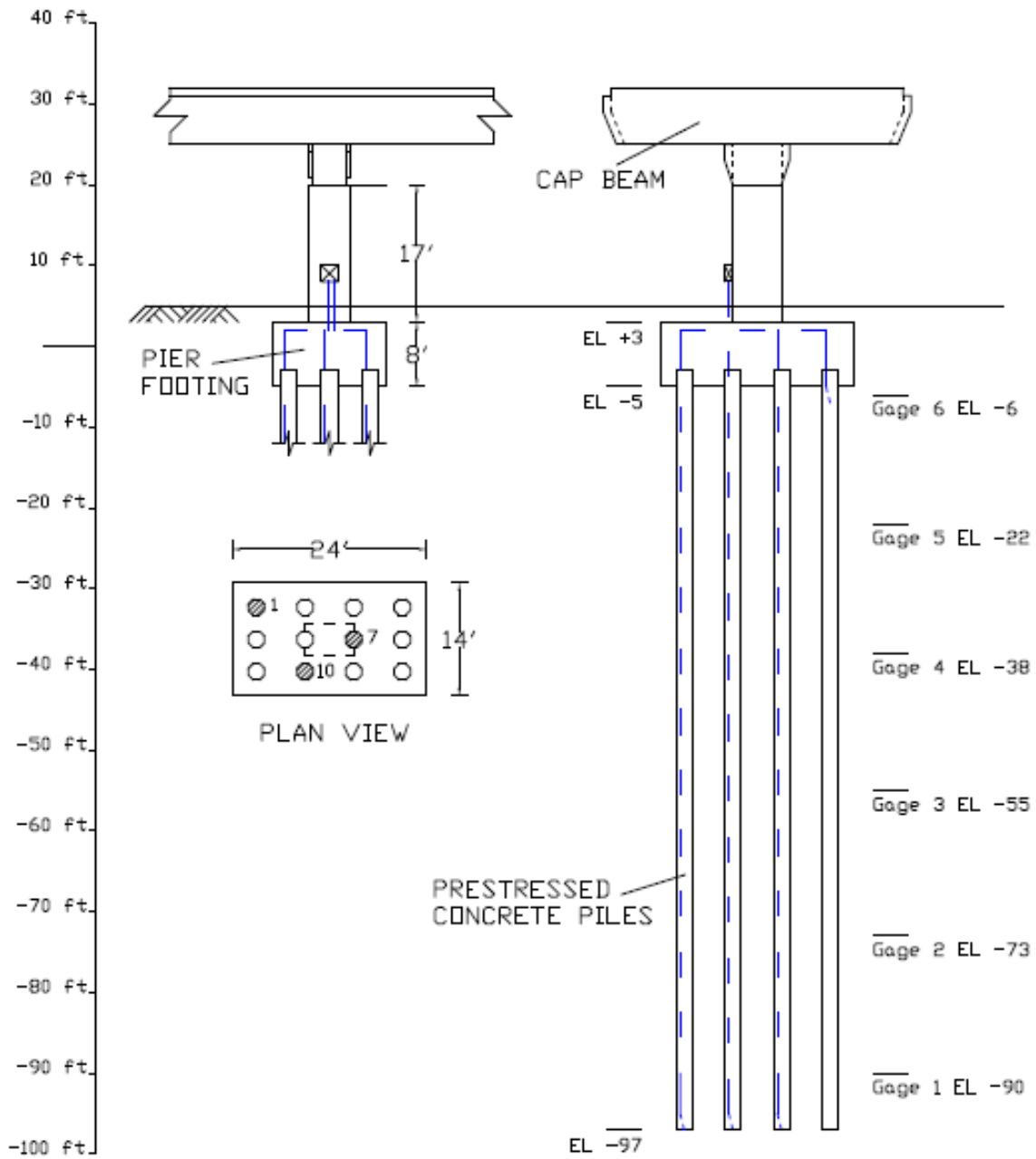
1 ft = 0.305 m

Figure 3. Illustration. Pier EA-31 pile instrumentation layout.

Table 1. Summary of gauge failures.

Gauge		Date of Failure
Quadrant 1/pile 7 pile tip load cell transducer 5194		Damaged during driving
Rod extensometer anchor (pile 1, anchor 1)		Failed during installation
Strain gauges	1-1-A	7/1999
	1-1-B	9/1988
	1-3-B	7/1999
	1-4-A	7/1999
	1-4-B	7/1999
	1-5-B	7/1999
	1-6-A	3/2002
	7-1-A	10/1987
	7-1-B	7/1999
	7-5-A	12/1984
	7-6-A	7/1999
	10-1-A	7/1987
	10-1-B	10/1987
	10-4-A	7/1999
	10-4-B	10/1993
	10-6-A	7/1999
	10-6-B	7/1999

Note: At the 20-year mark, 17 of the 62 gauges (27 percent) were not functioning. In addition, 17 of the 36 underwater gauges were not functioning at the 20-year mark.

As reported, all pile tip load cells were functioning after 20 years of service, with the exception of one transducer from pile 7, which was damaged during pile driving. From the data collected in 2002, the average load for all three piles was 94 tons (85.26 Mg) with a maximum deviation of approximately 11 percent (see 1 ton = 0.907 mg

figure 4). This data suggest that some eccentricity was present wherein slightly more load was being taken by the eastern-most piles (represented by pile 1).
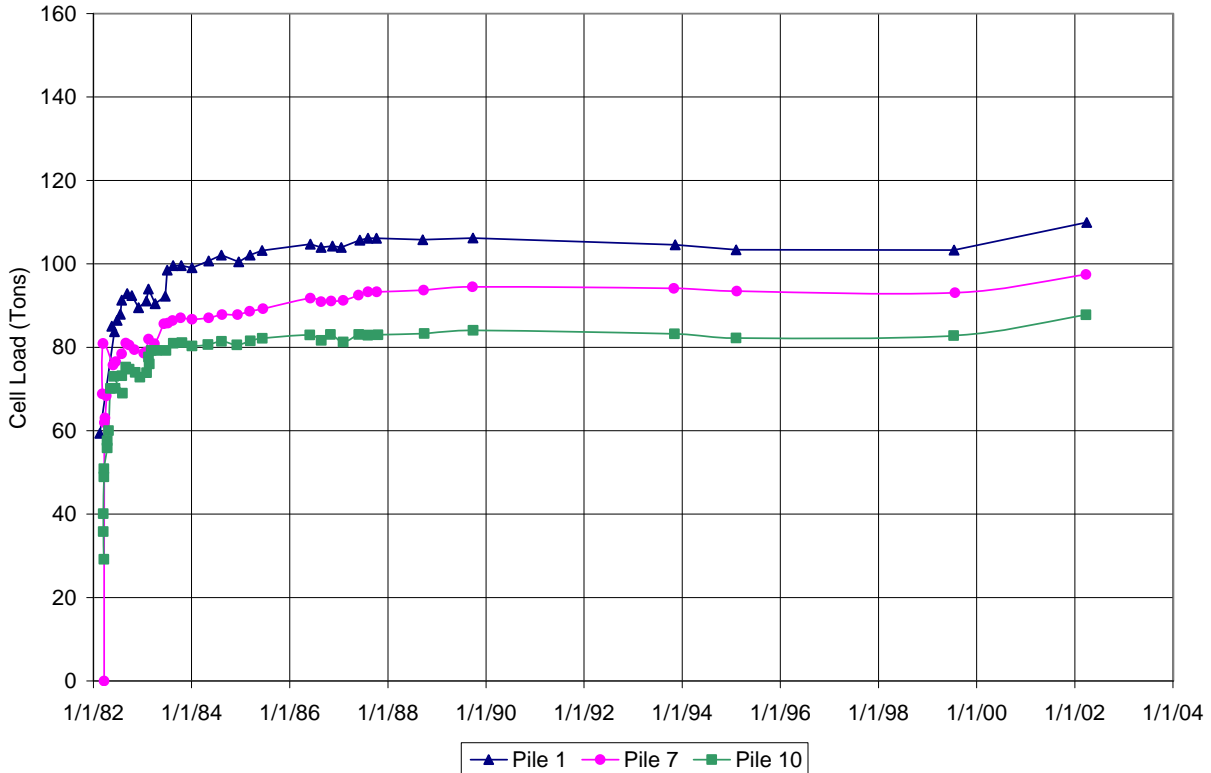
Figure 4. Graph. Pier EA-31 tip load in 3 of the 12 piles.

1 ton = 0.907 Mg

During the instrumentation phase, pairs of strain gauges were installed into the three monitored piles at six different levels along the pile. This provided 12 gauges in each pile for a total of 36 strain gauges. All of these gauges were located beneath the groundwater level, and 17 of these gauges were no longer functioning after 20 years of service. However, all the gauges were reported to have worked until at least October 1987, which provided 4 years of data collection. Since all of the gauges were installed below the groundwater level, it is possible that their failure was due to the water resistance of the system. The data from the strain gauges that were still in commission were plotted over time (figure 5 through figure 7).[1] For piles 1 and 10, the average strain change in the pile was between -300 and -500 µe (microstrain), with pile 1 being on the higher end of that range. However for pile 7, the average strain change in the pile was approximately -225 µe. This suggests that the piles further away from the center of the pile cap where the column is sitting experienced more strain change likely due to bending. The gauges installed at the top of the other piles and the strain gauges in the column were all still functioning after 20 years.
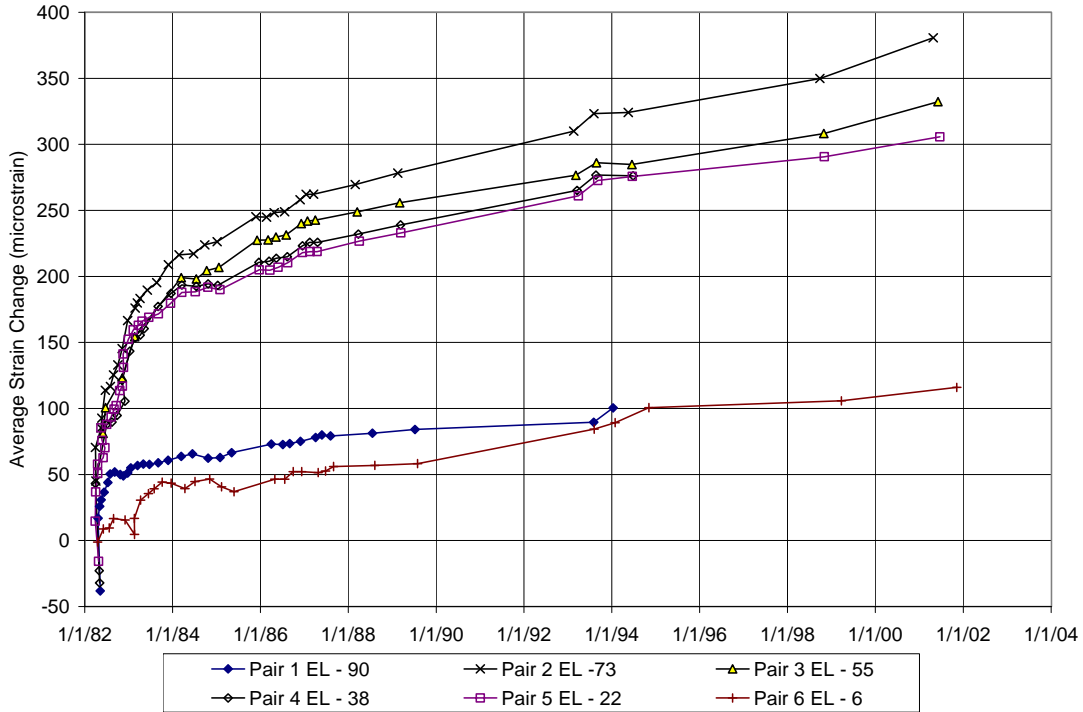
Figure 5. Graph. Pier EA-31 average strain change pile 1.
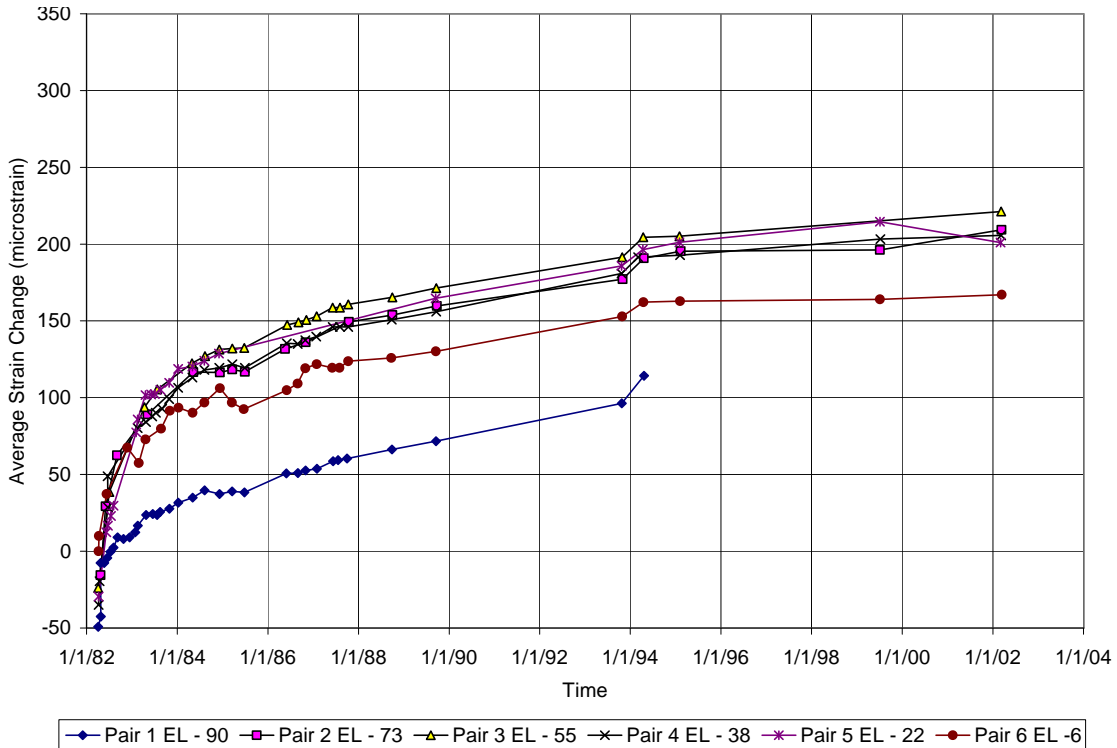
Figure 6. Graph. Pier EA-31 average strain change pile 7.
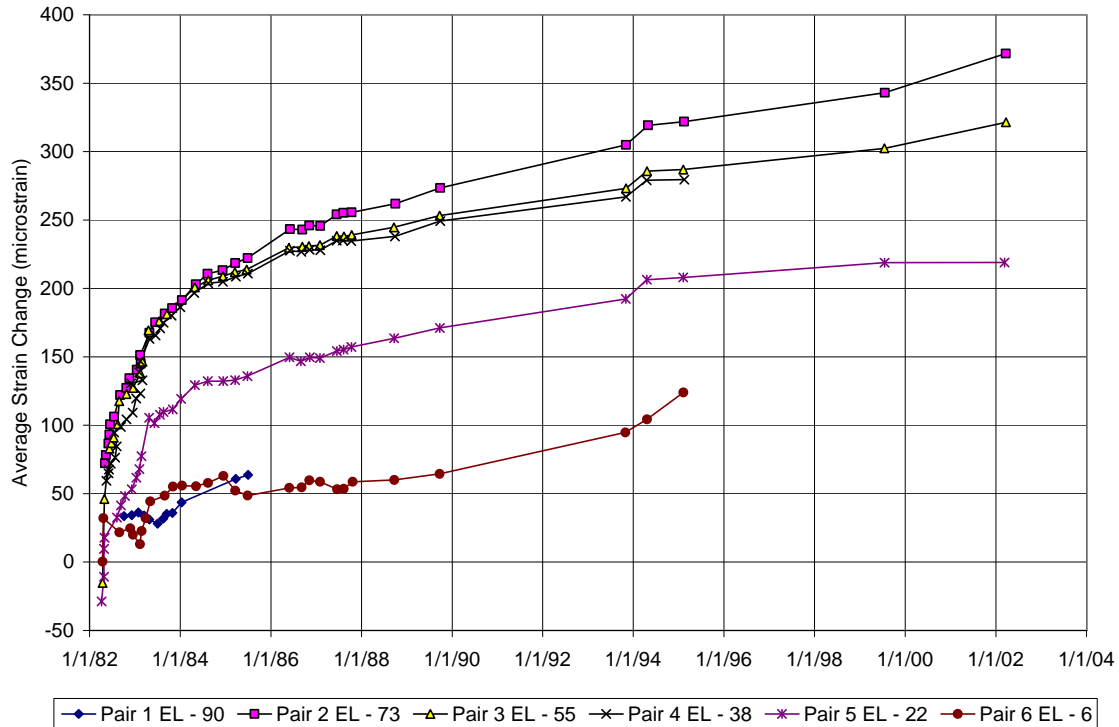
Figure 7. Graph. Pier EA-31 average strain change pile 10.

This study showed that SSHM using wired gauges is extremely useful. With the advances in the durability of data collection and monitoring systems, it is likely that this same system, if installed today, would not have the number of failed gauges. While this study required a worker to be onsite to record the data, the usefulness of the instrumentation provided insight into the design of foundations and instrumentation. While the technology record-keeping used in this study is somewhat outdated, the types of instrumentation are readily applicable and available (in a more robust form) for future studies. Automated data acquisition, monitoring, and remote data recovery are also available for this type of instrumentation and could be easily retrofit to the existing gauges.

WIRELESS SENSORS FOR HEALTH MONITORING

Wireless instrumentation has two connotations: (1) truly wireless gauges that minimize or even eliminate wiring attached to instrumentation, which is the topic of this section and (2) wireless communication (cellular or satellite) with instrumentation that may or may not employ onsite gauge wiring between the transducers and the data logger. Remote monitoring in itself is not automatically wireless, but rather, it may make use of landline communication between the data logger and querying parties.

Wireless systems use basically the same measurement devices (or transducers) as wired systems, but they use a transmitter and receiver system instead of lead wires. Wire costs range between $0.40 and $1.00 per 1 ft (0.305 m) per gauge and may require even greater expenses depending on the complexity of the installation site. Transmitters, similar to data logging equipment, are limited by their sampling and transmission rates—higher sampling rates come at higher costs with an upper rate limit of $5,000 to $10,000 samples/channel. The cost comparison of wireless

11

to wired systems is generally site specific, but it leans toward wired systems. However, in the case of moveable structures or mechanical devices, slip rings or other features which allow the movements of the wires are required and tend to tip the scales in favor of wireless systems.

Wireless sensors for SHM systems are used more frequently as the technology becomes more available. Since no wires are required between the gauges and the DAS, installation time and associated costs are reduced as compared to traditional wired systems. Typically, wireless sensors are installed over an entire structure to get a full mapping of the desired measurement (i.e., stress, strain, displacement, temperature, velocity, etc.) across the entire structure. A wireless DAS collects the data sent back from these sensors and stores the collected data to an onsite data logger. As with most health monitoring programs, almost all wireless instrumentation used to-date involve superstructure and not substructural elements.

A study by Arms et al. introduced the idea of a SHM system in which the data acquisition software could be reprogrammed remotely.[2] The goal was that the operating parameters of a monitoring system, such as sampling rate, triggering parameters, downloading intervals, etc., should be alterable from a remote location. As a result, operators should never have to go back to the site after initial installation. This provides a fully remote monitoring system in which all the parameters of the data logging and collection can be altered from a separate location.[2]

The wireless transmittable gauges were installed on the existing structure at main points of interest. Wireless sensors received transmitted data, and the data were uploaded to an onsite laptop (see figure 8). The laptop transmitted the data through a cellular uplink to the base station. From this base station, the software on the laptop could be altered to change the data collection parameters. The software could also be altered with trigger parameters so that the system could be sleeping but would wake up when an event occurred that increased the change in strain levels, such as a train crossing a bridge (see figure 9).

Figure 8. Photo. Wireless data collection and transmit setup.[2]

Figure 9. Photo. Train crossing bridge causing a strain event.[2]

While the software allows for a completely wireless system, its use as a SSHM system is not as probable. For installation in the deep foundation system, wireless sensors would have to be extremely powerful to transmit data wirelessly through surrounding soil, sometimes at depths of 100 ft (30.5 m). Even if they were available, sensors capable of this would most likely be too expensive to negate the cost savings from not using wired sensors. Furthermore, sensors used for reinforced concrete structural elements can provide much better data when installed within the concrete member where the reinforcement is located. Once again, a typical wireless sensor would not have the capability to transmit signals through hardened concrete. However, the wireless DAS could still be used with no obstructions.

Systems that overcome deep concrete embedment that are presently used are quasi-wireless where gauges are installed deep within the structure tethered to a transmitter at the concrete surface. These systems still suffer from power draw, and the useful unattended lifespan is limited, especially at high-sampling and transmission rates.

Susoy et al. researched the development of a standardized SHM system for the movable bridges in Florida.[3] The assumption was that due to the multitude of elements, movable bridges were more prone to damage and deterioration and that the typical visual inspection as required by FHWA was not adequate. The study detailed the SHM system that was installed on the SR-401N Bascule Bridge over the Barge Canal in Port Canaveral, FL (see figure 10 and figure 11). A detailed finite element analysis was run to determine the probable locations for stress concentrations on the bridge. Once this was complete, wireless transmitting strain gauges were mounted on the bridge in these locations (see figure 11). The strain sensors transmitted their data wirelessly to the installed DAS, and the data were logged on a field computer also installed onsite.[3]
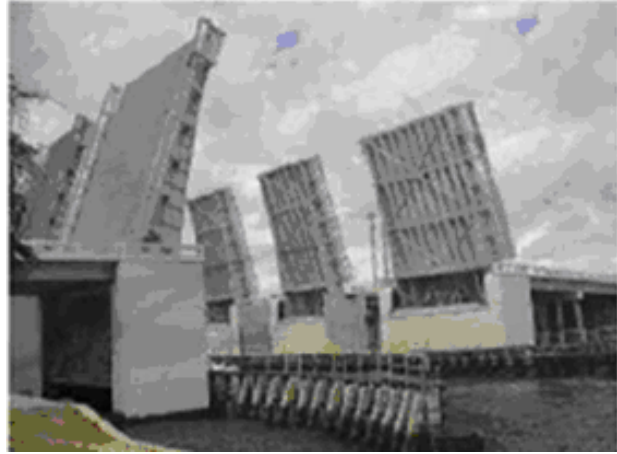
Figure 10. Photo. Bascule Bridge on SR-401N in Port Canaveral, FL.[3]
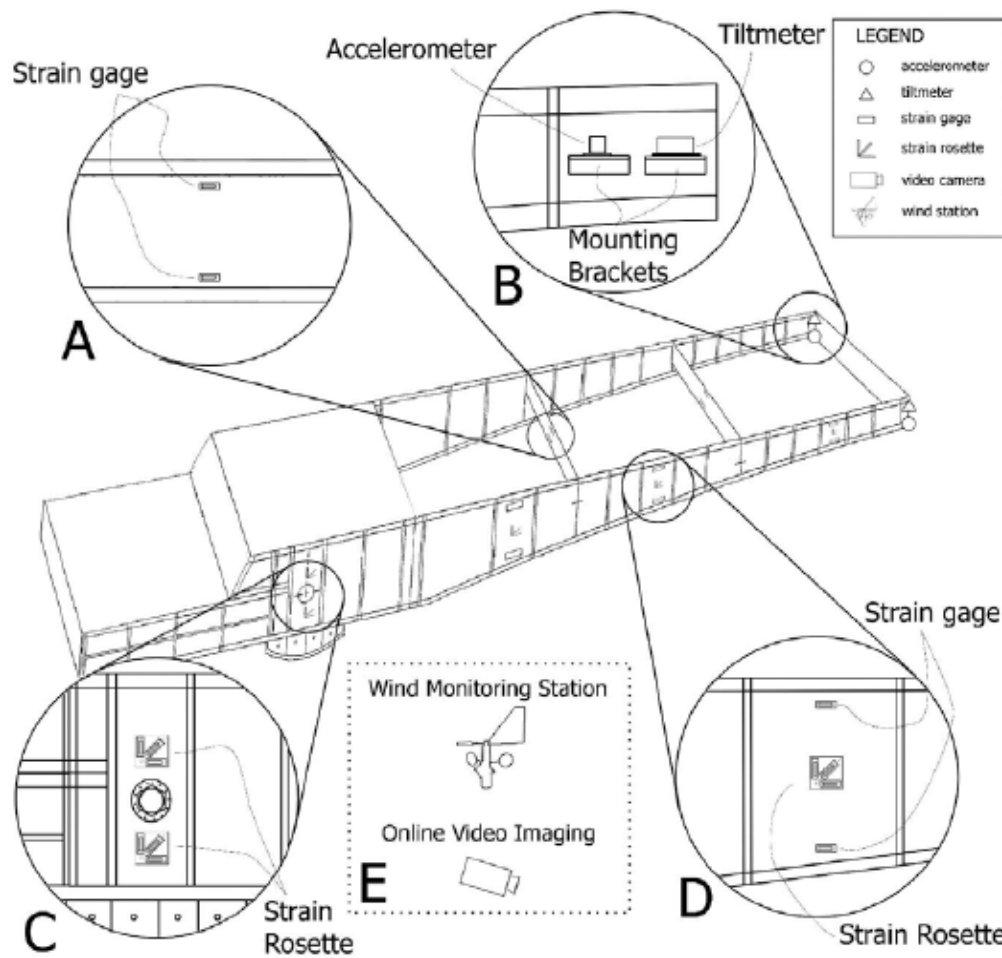
Figure 11. Illustration. Locations and types of sensors on Bascule Bridge.[3]

For this study, the wireless sensors were almost a necessity due to the type of project. Installing wired sensors on a movable bridge could prove to be difficult and cause damage to the wires. No mention was made concerning the accessibility of the data once they were collected, so it is assumed that the data were downloaded by a worker sent to the site. However, this study was

based on the idea of wireless sensors for the monitoring system and therefore would have the same difficulty translating to SSHM as the Arms study.[2]

A study by Watters et al. introduced the idea of a special design for a wireless sensor capable of detecting threshold levels.[4] The sensor was coupled with a radio frequency identification (RFID) chip. The sensor is read by scanning the system with a radio frequency (RF) transceiver. The RF transceiver alerts the RFID chip to power the sensor to collect data. Once the data are collected, the RFID chip transmits the data back to the transceiver to be read.[4]

The study focused on the use of the sensor to determine whether certain data may have crossed a threshold, namely chloride ingress into reinforced concrete structures. A particular threshold was set, and the system read the data and determined if the threshold had been met. The system was extremely useful for data that did not need to be streamed. For chloride intrusion into reinforced concrete structures, the critical point at which the chloride concentration is reached could take years to be met. Therefore, a DAS capable of collecting and logging data at a high rate was not needed. In typical concrete inspection, a core sample of the concrete deck must be taken and analyzed in a lab. With this technology, a sensor can be embedded into a structure and then routinely checked at a predetermined interval. Furthermore, the trends can be plotted over time to help owners and engineers predict when the chlorine intrusion will reach a critical level. The capability to send an alert when a certain threshold level is reached would be extremely useful in bridge monitoring. If an alert is programmed into the transducer that reacts when a certain level is met, it will allow authorities to react and make a decision about keeping a bridge open or closing it down depending on the severity of the event, which may save lives.

While this is a useful system for data that need to be monitored over long intervals, from a SHM point of view, the system is not beneficial for structures loaded with highly irregular or dynamic loading, such as a bridge. The sensors for a bridge SHM system would need to be read and have the data collected and stored at a relatively high rate in order for the owner or engineer to determine what is happening to the structure during its service life.

FIBER OPTIC SENSORS FOR HEALTH MONITORING

With the recent advances in the telecommunications field with fiber optics, the interest in fiber optic sensors (FOSs) has increased and has made way for powerful new sensors to be used for SHM. FOSs send light beams through the fiber optic cable at regular intervals and measure the return time. When the cross sectional area of the cable changes, the return time changes. This change in return time can be related to engineering parameters (i.e., strain, displacement, etc.) of the structural member to which they are attached. They are considered to be beneficial because they are relatively immune to interference from radio frequencies, electric or magnetic fields, and temperature differences.

A study by Udd et al. introduced the use of FOSs in existing structures.[5] The study introduced single-axis fiber grating strain gauges for the use of nondestructive evaluation of existing structures. The benefits of these include a long service life and the fact that they can be installed in long gauge lengths, providing more accurate results. There was nothing in the study that related to remote or wireless monitoring; it focused on the sensitivity of the gauges as well as the installation requirements of working on an existing structure.

In this case, the bridge required structural strengthening in order to accommodate increased loads on the structures that were not expected at the time of construction. The bridge was strengthened using fiber-reinforced polymer (FRP) composites that did not alter the appearance of the bridge while still providing increased strength (see figure 12).[5] The fiber grating strain gauges were installed by embedding them into saw cuts in the bottom of the bridge girders and on the outside of the adhered FRP coating (see figure 13 and figure 14).[5]

Figure 12. Photo. FRP wrap installation on bridge superstructure.[5]

Figure 13. Photo. FOS installation on bridge superstructure.[5]

Figure 14. Photo. FOS installation over FRP wrap on bridge superstructure.[5]

The Udd et al. study focused primarily on the monitoring of the bridge superstructure, but the FOSs could have been installed just as easily to the pile foundation of the bridge.[5] This would have provided data showing how the bridge foundation reacted to the same loads that were visible in the data from the superstructure. The sensors proved to be sensitive. The gauges detected not only small cars crossing the bridge, but also, on one occasion, the effect of a single person running out to the center of the bridge, jumping up and down five times, and walking back off the bridge (see figure 15). Furthermore, gauges were easily installed by embedding them within the structure and applying them to the exterior of the structure with adequate results from each installation.
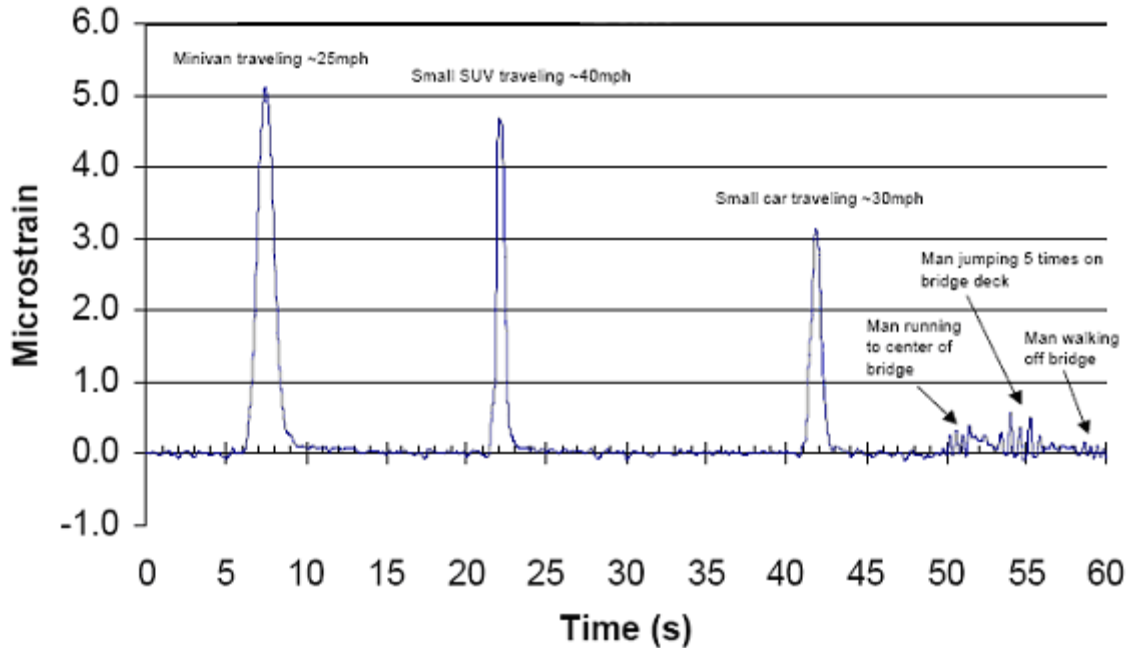
1 mi = 1.61 km

Figure 15. Graph. Measurement of strain induced on bridge from varying events.[5]

FOSs are helpful in a SSHM system because of their relative immunity to temperature effects. Typically, bridge foundations are designed with mass concrete elements such as drilled shafts or piles for the subsurface foundation, a shaft or pile cap, and large concrete columns. The temperature changes that can take place inside these mass concrete elements are large. Typical vibrating wire gauges show large frequency changes due to temperature that must be corrected when analyzing. Fiber optics results showed only the strain that is truly induced by temperature change in the structure and not that of the gauges.

A study by Hemphill examined the combining of wireless technology with FOSs.[6] The study proposed and tested the idea of a fully integrated continuous wireless SHM system for the East 12th Street bridge in Des Moines, IA (see figure 16). Fiber bragg grating (FBG) strain sensors were installed at 40 different locations on the bridge. The data collector scanned the FBG sensors and transmitted the data wirelessly to a computer in a secure facility close to the site (see figure 17). The data were stored as a data file and automatically uploaded to a file transfer protocol (FTP) site. When this site was accessed, the data file was downloaded and deleted from the FTP site to make room for the next data file. These data were compiled, processed, and posted to a Web site that allowed users to view real-time strain data along with real-time streaming video of the bridge.[6]

Figure 16. Photo. East 12th Street bridge in Des Moines, IA.[6]

Figure 17. Photo. Host computer near East 12th Street bridge site.[6]

This system is useful because it provides the end user with simple, easy-to-follow data viewing that is easily monitored. With the addition of the real-time streaming video, a data monitor can review the data, compare them with the live traffic on the bridge, and make the necessary correlations to the loading on the structure. The wireless transmitting of the data is also useful because it reduces the man hours that are normally required to go to the site and download the data from the collection system, which can be time consuming and expensive. This system is efficient and has few drawbacks, if any. The FOS gauges can be installed in the substructure and on the superstructure, and there are no limiting factors to the system.

CURRENT AND FUTURE POSSIBILITIES FOR HEALTH MONITORING

Weyl summarized the proposal for a full-scale SHM system for the Indian River Inlet Bridge in Delaware.[7] The design of the SHM system was fully integrated throughout the design phase of the project so that it fit seamlessly with the construction phase. The following types of gauges were installed throughout the bridge: vibrating wire strain gauges, weldable foil strain gauges, accelerometers, global positioning system sensors, load cells, linear potentiometers, corrosion monitors, etc. This creates a total of 240 sensors, 11 DASs, and 39 data loggers.[7]

The project will be carried out in three phases. Phase I took place during construction to determine live construction loads. Phase II will take place immediately after bridge construction to determine the initial response of the bridge to traffic, thermal, and wind loading. Phase III will take place during the intended service life of the bridge to compare against the data collected during phase II.[7]

Finally, a Web-based user interface was developed to present data in an easy-to-read and understandable format for the University of Delaware, the Delaware Department of Transportation, and those that worked on the project. At the time of this report, there were no data to report from this project because it was still in the preliminary construction phase.

This project provides an example of the future possibilities that SHM holds for the sustainability of the Nation's infrastructure. Fully integrating the monitoring system into the design phase of the project does not delay construction or hold back the monitoring system. The data collected from this type system can be archived as data that are useful for the history of the bridge and that help with the determination of any possible problems that might occur.

This particular study involved a high number of sensors, gauges, and DASs for the full SHM system, but it is still similar to the proposed monitoring for the I-35W bridge monitoring system that is studied in this report. The use of everyday technology, such as a Web site that provides interested users with real-time data from the bridge, coupled with the advanced technology of resistance and vibrating wire strain gauges, will propel SHM systems into practice.

CHAPTER 3. VOIDED SHAFT THERMAL MONITORING

The first remote monitoring effort conducted during this study involved the thermal monitoring of a drilled shaft. Florida's bridge substructures have continually grown in size due to the high demand of larger bridges to accommodate the growing population. Typically, drilled shafts were not considered to behave as a mass concrete element due to their smaller size (usually no greater than 4 ft (1.22 m) in diameter). However, with the increase in size of today's bridge foundations to accommodate longer spans with reduced numbers of collision-prone piers, common sizes of drilled shafts are larger and act as mass concrete elements (such as the 9-ft (2.7-m)-diameter shafts for the Ringling Causeway Bridge in Sarasota, FL). Until recently, these larger diameter shafts have slipped through the concrete specifications without special review for mass concrete effects. Aside from the more widely recognized differential temperature concerns, an equally important issue is the high temperatures that occur during the curing of mass concrete elements. Therein, the delayed ettringite formation can lead to long-term durability reduction where internal cracking initiates in regions that experience elevated curing temperatures.

To combat mass concrete effects in large diameter drilled shafts, researchers at the University of South Florida (USF) in Tampa, FL, proposed and constructed a drilled shaft with a full-length centralized void to mitigate the mass concrete effects exhibited by the foundation element. Benefits from this approach were twofold: (1) to eliminate mass concrete effects in large diameter drilled shafts and (2) to reduce the concrete volume and cost required to construct these foundation elements.

This chapter focuses on the remote thermal monitoring procedure that was used for the research conducted on the USF voided shaft research project. Of particular interest is the installation and instrumentation of the drilled shaft, the thermal monitoring procedure and a review of its efficacy, and the results from the remote thermal monitoring system and its individual parts. More emphasis is placed on the actual monitoring procedure than the results from the voided shaft; however, these thermal results are presented in a summary.

TEST SPECIMEN INSTRUMENTATION

The testing site for the thermal monitoring of the voided shaft was in Clearwater, FL, at the equipment yard (see ©2008 **google®**

figure 18).
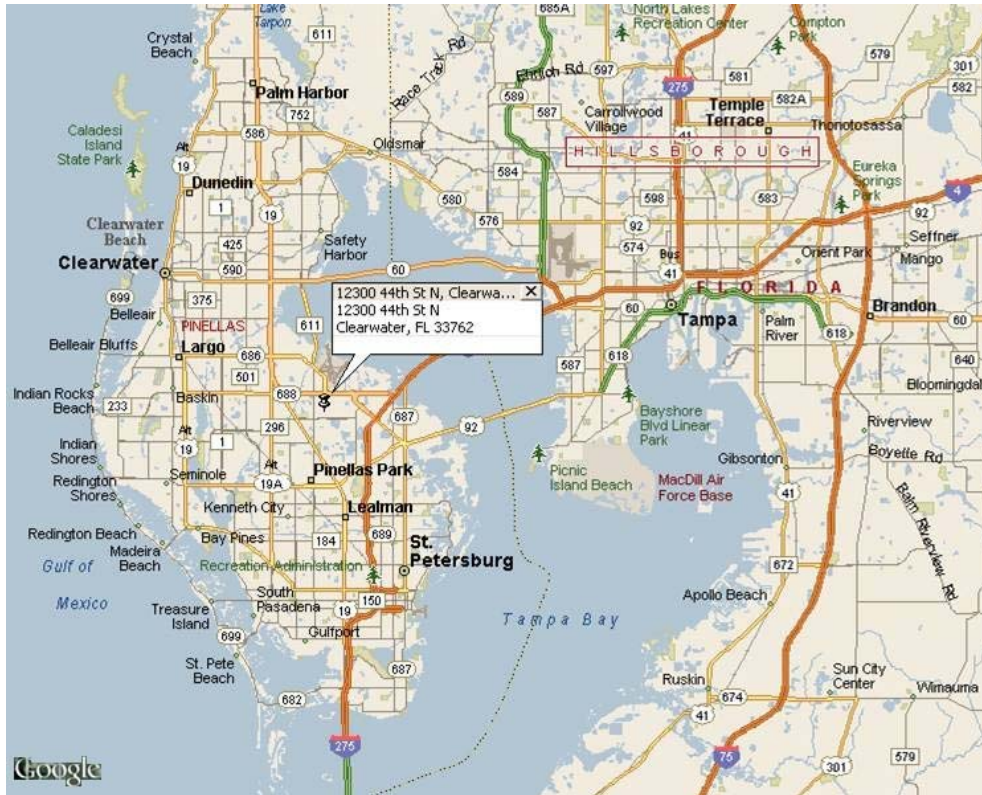
©2008 Google®

Figure 18. Illustration. Map of voided shaft testing site.[8]

Prior to the construction of the drilled shaft, the instrumentation for the thermal monitoring was put into place. The first step was the instrumentation of the rebar cage that was installed in the shaft. The reinforcement cage was built using 36 longitudinal bars with 26 #5 stirrups at 12 inches (304.8 mm) on the center. The cage was equipped with nine Schedule 80 polyvinyl chloride (PVC) pipes for thermal testing, which were 26 ft (7.93 m) long and 2 inches (50.8 mm) in diameter (see figure 19). On three of these tubes at 120-degree spacings from each other, thermocouples (TCs) were placed at the top, middle, and bottom of the tubes to provide readings from around the shaft. The inner steel casing (needed to provide the central void in the shaft) was outfitted with three crossbar supports welded to the interior of the casing, which allowed for a central tube to be run through the center of the void for thermal integrity testing (see figure 20). TCs were also placed at the top, middle, and bottom of each side of the inner casing spaced 120 degrees away on the crossbars and attached to the top, middle, and bottom of the central tube (see figure 21). More TCs were placed at the top, middle, and bottom of the outside of the inner casing (see figure 22). In the surrounding soil, ground monitoring tubes were installed at distances corresponding to fractions of the shaft diameter (D); 0.25D, 0.50D, 1D, and 2D away from the edge of the shaft (see figure 23). TCs were also installed with the tubes at these locations.

22

Figure 19. Photo. Voided shaft reinforcement cage instrumentation.

Figure 20. Photo. Voided shaft center casing center tube supports.

Figure 21. Photo. Voided shaft TCs installed in center casing.

Figure 22. Photo. Voided shaft TCs on outside of center casing.

Figure 23. Photo. Voided shaft ground monitoring tube installation.

TEST SPECIMEN CONSTRUCTION

The voided shaft was constructed at the test site on September 25, 2007. The entire construction process was broadcast via webcam from the USF geotechnical Web page for those who were unable to visit the construction site. Records of the construction sequence, thermal testing, and long-term thermal monitoring were posted and updated every 15 min to http://geotech.eng. usf.edu/voided.html. A 9-ft (2.7-m)-diameter drilled shaft with a 4-ft (1.2-m)-diameter central void was constructed. The first step was the excavation; an oversized surface casing 10 ft (3.05 m) in diameter and 8 ft (2.4 m) in length was embedded 7 ft (2.1 m) into the soil. Excavation was carried out in the dry condition with a 9-ft (2.7-m)-diameter auger for the first several feet. After which, polymer slurry was introduced into the excavation for stabilization. The excavation proceeded without issue to a depth of 25 ft (7.6 m) (see figure 24). A cleanout bucket was used to scrape the bottom of the excavation of debris immediately after the auger and then again after a 30-min wait period.

Figure 24. Photo. Excavation for voided shaft.

The reinforcement cage was picked at two locations to avoid excess bending (see figure 25). Locking wheel cage spacers were placed along the length of the reinforcement cage to maintain 6 inches (152.4 mm) of clear cover (see figure 26). The reinforcement cage was hung in place during the pour so that the finished concrete was level with the top of the cage (see figure 27).

Figure 25. Photo. Picking of reinforcement cage for voided shaft.

Figure 26. Photo. Placement of reinforcement cage for voided shaft.

Figure 27. Photo. Hanging of reinforcement cage for voided shaft.

The central casing used to create the full-length void had a 46-inch (1,68.4-mm) outer diameter steel casing that was 30.5 ft (9.3 m) long. It was set into the center of the excavation with a crane (see figure 28 and figure 29). The self weight of the steel casing penetrated the soil to about 3 to 6 inches (76.2 to 152.4 mm). This prevented the concrete from entering the void area. To prevent the top of the inner casing from shifting during the initial concrete pour, a back-hoe bucket was used to hold the top of the casing steady (see figure 30). A double tremie system was used to place the concrete on opposite sides of the excavation (see figure 31). Concrete specifications were a standard 4,000 psi (27,560 kPa) with an 8-inch (203.2-mm) slump and #57 stone mix design. During the concrete placement, concrete level at three points around the shaft was measured to ensure that the concrete was flowing around the void and through the reinforcement cage. The temporary surface casing was removed after final concrete placement (see figure 32 and figure 33).

Figure 28. Photo. Picking of central casing for voided shaft.

Figure 29. Photo. Placement of central casing for voided shaft.

Figure 30. Photo. Holding of central casing steady for voided shaft.

Figure 31. Photo. Double tremie concrete placement of voided shaft.

Figure 32. Photo. Voided shaft outer steel casing removal.

Figure 33. Photo. Final voided shaft at ground level.

MONITORING SYSTEM INSTRUMENTATION AND PROCEDURE

Once the construction of the voided shaft was complete, all of the TC wires were accessed through the tubes so they could be attached to the data collection system. The remote monitoring system was composed of several parts: A Campbell Scientific, Inc.® CR1000 data logger, an AM25T 25-channel multiplexer, a Campbell Scientific, Inc.® Raven100 CDMA AirLink cellular modem, PS100 12-V power supply and 7-Ahr rechargeable battery, a 12W Solar Cell panel from Unidata, and a large environmental enclosure to protect all the materials from the elements (see figure 34 through figure 38). The total cost of the system including all equipment and ongoing services was approximately $4,500. The TC wires were connected to the multiplexer because there were not enough channels on the CR1000 to read all of the TCs. The multiplexer was then connected to the CR1000 (see figure 39). LoggerNet, the remote monitoring and data collection software from Campbell Scientific, Inc.®, was used to program the CR1000 for remote monitoring and data recovery. The data collection system was equipped with the solar panel to help sustain the battery voltage (see figure 40). The system was programmed to wake up every 15 min, take a temperature reading, record it, and go back to sleep. The Raven100 modem was programmed to wake up once every 60 min and transmit the collected data back to the host computer for processing, which was stationed in the Geotechnical Research Group at USF. Sideline measurements of ground temperature for a companion study were taken 1D and 2D away from the shaft via an OMEGA® OM-220 data logger that collected data at the same rate as the CR1000; however, the data were simply stored, and a site visit was required to collect that data. The remote system's battery voltage was also monitored and sent to the host computer along with the thermal data so that the power consumption could be tracked.

Figure 34. Photo. Campbell Scientific, Inc.® CR1000 data logger.

Figure 35. Photo. AM25T 25-channel multiplexer.

Figure 36. Photo. Campbell Scientific, Inc.® Raven100 CDMA AirLink cellular modem.

Figure 37. Photo. Campbell Scientific, Inc.® PS100 12-V power supply with rechargeable battery.

Figure 38. Photo. Campbell Scientific, Inc.® ENC12x14 environmental enclosure.

Figure 39. Photo. TC wire connection from AM25t 25-channel multiplexer to CR1000 data logger.

Figure 40. Photo. Remote thermal monitoring system for voided shaft.

RESULTS AND CONCLUSIONS

Overall, the system worked well. At one point during the monitoring period, there was a cellular timeout, and the modem stopped transmitting the data to the host computer. This was fixed by a

site visit to reset the modem, and the problem did not occur again. However, the main problem that was encountered was an issue with power usage. At the beginning of the monitoring procedure, the Raven modem was left on and sent back data every hour, which used a large amount of power, and the system lost power after a few hours (see figure 41). The monitoring procedure was revised so that the modem would go to sleep and only wake up once every hour to transmit the collected data. Even with this alteration, the battery was still losing power relatively quickly. Once the battery voltage dropped below 11.6V, the data collection system had approximately 8 h of life before it quit. Due to this large amount of power usage, three site visits were required to recharge the battery. These visits are seen in the plot of the battery voltage over time (see figure 42). In order to provide a completely remote unit, a larger solar cell was recommended because the 12W did not provide enough power to make the system fully remote.
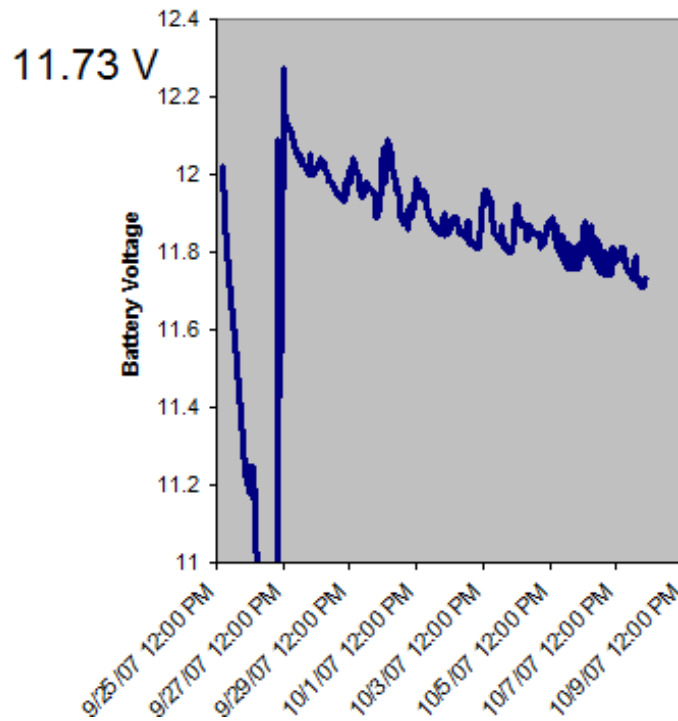
Figure 41. Graph. Battery voltage of thermal monitoring system as of October 8, 2007.
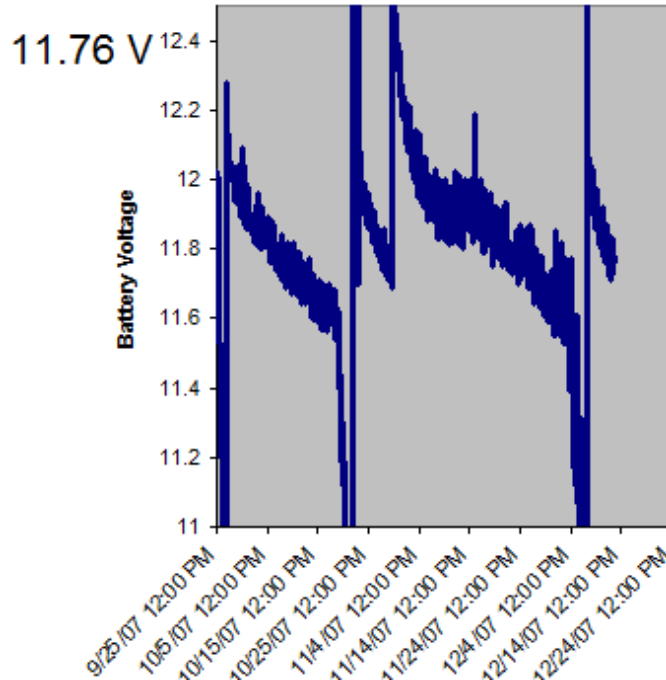
Figure 42. Graph. Battery voltage of thermal monitoring system as of December 14, 2007.

Originally, the data collection period was supposed to last until the temperature in the shaft had reached equilibrium. However, in reviewing the data, the temperatures recorded from the soil surrounding the shaft were increasing while the temperatures within the shaft had reached equilibrium (see figure 43). Therefore, data collection continued for another period of time until it was determined that the temperatures both in the shaft and in the surrounding soil had reached equilibrium. From the final temperature plot, it is evident that the temperature in the soil 1D away from the shaft was the last to eventually reach equilibrium. It can also be seen that the temperature in the soil at 2D away from the shaft was affected only slightly by the heat coming from the shaft (see $°f = 1.8(°c) + 32$

figure 44).

$°F = 1.8(°C) + 32$
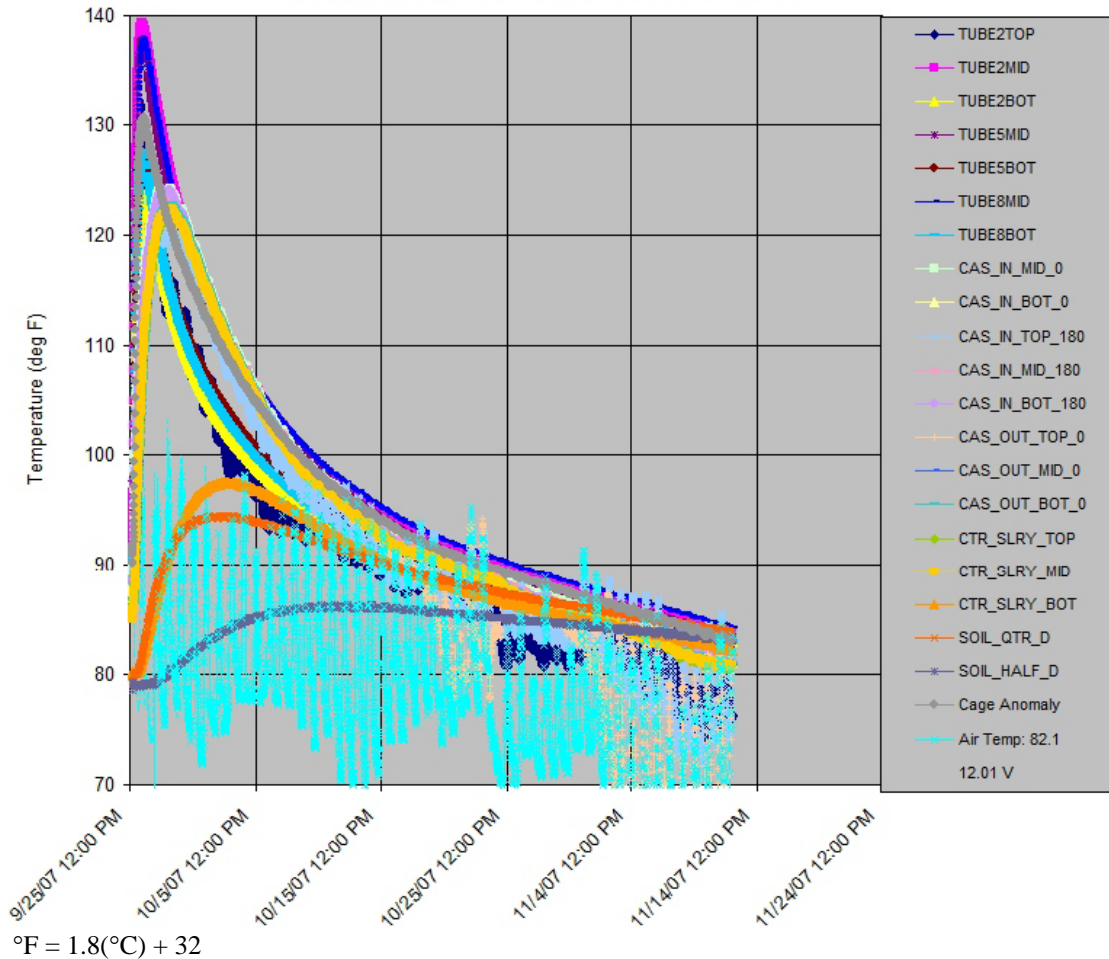
Figure 43. Graph. TC data from voided shaft as of November 12, 2007.

°F = 1.8(°C) + 32
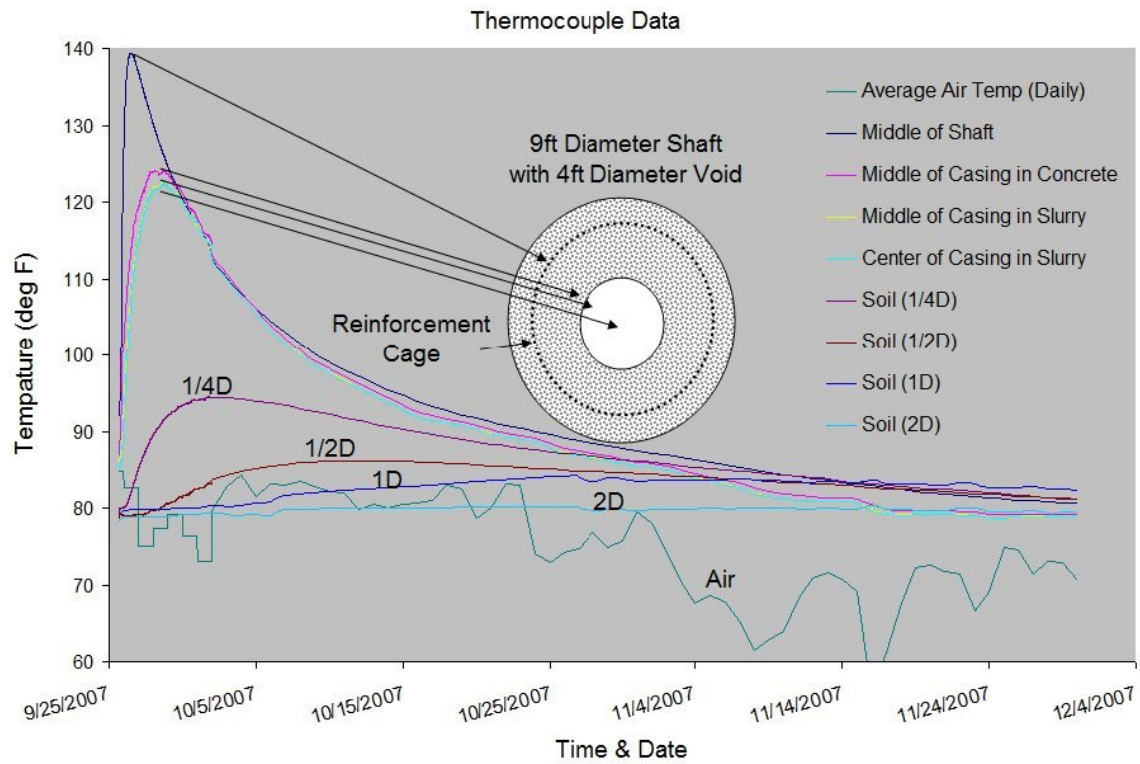
Figure 44. Graph. Final average TC data for all locations.

CHAPTER 4. I-35W BRIDGE FOUNDATION MONITORING

On August 1, 2007, the I-35W bridge over the Mississippi River in Minneapolis, MN, collapsed in the middle of rush hour. The collapse killed 13 people and revealed to engineers the United States' failing infrastructure. Part of this study proposes that a catastrophe such as this may be prevented through the use of remote monitoring systems with the capability to alert users when certain structural members reach a predetermined level of stress. In order to fully understand the forces induced into a structure such as a bridge, the Minnesota Department of Transportation (MnDOT), FHWA, the USF Geotechnical Research Group, and Foundation & Geotechnical Engineering (FGE), LLC teamed to provide a remote monitoring system that would provide much of this information. As MnDOT rebuilt I-35W, a number of substructural members provided real-time information about the stresses on the bridge. Figure 45 shows the pier selected to demonstrate the monitoring system.
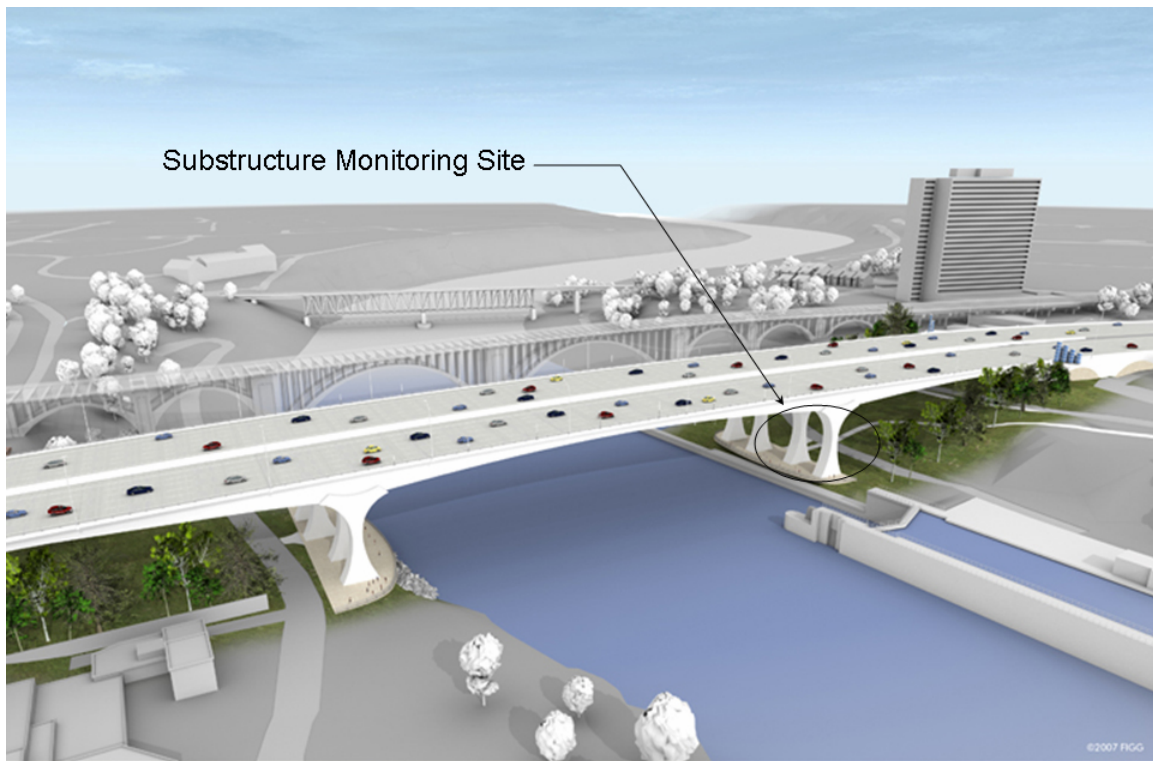
Figure 45. Illustration. I-35W bridge over the Mississippi River.

This study was broken into three phases: (1) real-time monitoring of the mass concrete effects in the drilled shaft foundation elements, (2) real-time monitoring of construction loads transmitted first into the drilled shafts and second into the columns as they came into play, and (3) long-term monitoring of the bridge loads and performance.

The first phase occurred during the construction of the concrete drilled shafts or caissons and the pier footing that ties the drilled shafts together. TCs were placed in the rebar cages of the shafts and throughout the pier footing and were used to determine the core temperatures of the mass

concrete elements. This part of the study was similar to the voided shaft study that was discussed in chapter 3.

The second phase of the study slightly overlapped the first phase in that it involved the drilled shafts, but it also branched upward to the columns. Two different types of strain gauges were placed in the rebar cages of the shafts and at the center height of the columns. These were used to more accurately determine the load induced in the shafts by the pier footing, columns, superstructure, and the loads induced in the columns by the bridge superstructure during the bridge construction. Furthermore, as each new section of the concrete box-girder superstructure was added to the columns, the added weights of the sections were correlated to the strain in the columns measured by the installed gauges. This provided more accurate calibrations that were used in the ongoing health monitoring of the bridge, which was the third phase of the project.

The third phase uses the same strain gauges that were embedded in the shafts and columns, including the strain gauges that will be installed in the superstructure components of the bridge. The final phase of the project will monitor the loads on the bridge throughout its service life, which can be used to determine the structural health of the bridge and provide MnDOT and FHWA with real-time strain and load data from the bridge (see figure 46).

Event Schedule	Shaft Instrumentation	Shaft Construction	Shaft Concrete Curing	Footing Construction	Footing Instrumentation	Footing Concrete Curing	Column Lift 1	Column Lift 2	Column Instrumentation	Column Lift 3	Superstructure Construction	Bridge Completion	Long-Term Health Monitoring
Project Phase I	███	███	███	███	███	███							
Project Phase II				███	███	███	███	███	███	███	███		
Project Phase III												███	███

Figure 46. Illustration. Event schedule and overlap of I-35W bridge project phases.

PHASE I—THERMAL MONITORING

As stated previously, in phase I, researchers monitored the internal temperatures of the mass concrete elements (drilled shafts and pier footing). While the overall procedure of the thermal monitoring was similar to the voided shaft study, there were some major differences. First, the shafts were solid and not voided. Second, the ambient temperature at the site was much different. As seen in figure 43 and °f = 1.8(°c) + 32

figure 44, in the Tampa Bay, FL, area during the monitoring period, the air temperature ranged from approximately 99.86 to 64.94 °F (37.7 to 18.3 °C). During the construction and thermal monitoring period in Minnesota, the temperature ranged from approximately 34.88 to -10 °F (1.6 to -23.3 °C). This was expected to have a significant
effect on the temperatures reached by the mass concrete elements.

Construction and Instrumentation

Prior to construction and installation of the drilled shafts, the instrumentation for the thermal monitoring was put into place. The first step of the placement was the instrumentation of the reinforcement cage for the drilled shafts. The reinforcement cage was built using high-strength longitudinal steel and mild stirrup steel. The cage had 2.48-inch (20.63-mm) threaded longitudinal bars with #6 bar circular ties at 5 inches (127 mm) on the center. Locking wheel cage spacers were placed along the reinforcement cage to maintain 6 inches (152.4 mm) of clear cover (see figure 47).

Figure 47. Photo. I-35W bridge shaft reinforcement cage construction.

After the reinforcement cages were assembled, they were instrumented with TCs and strain gauges. The strain gauges are discussed in the section on phase II. The TCs were installed in pairs at 4 levels along the shafts, later named GL1, GL2, GL3, and GL4, for a total of 10 TCs per shaft (2 TCs were installed in the center of the shaft near the top on a 20-ft (6.1-m) rebar placed after concreting). GL4 was located at the bottom of the shaft, GL3 was located at the top of competent rock, GL2 was located at the bottom of the permanent casing (top of weak rock), and GL1 was located at the top of the shaft (see figure 48). The wires from the TCs were bundled with the wires from the strain gauges and run to the top of the shafts in two groups (see figure 49).
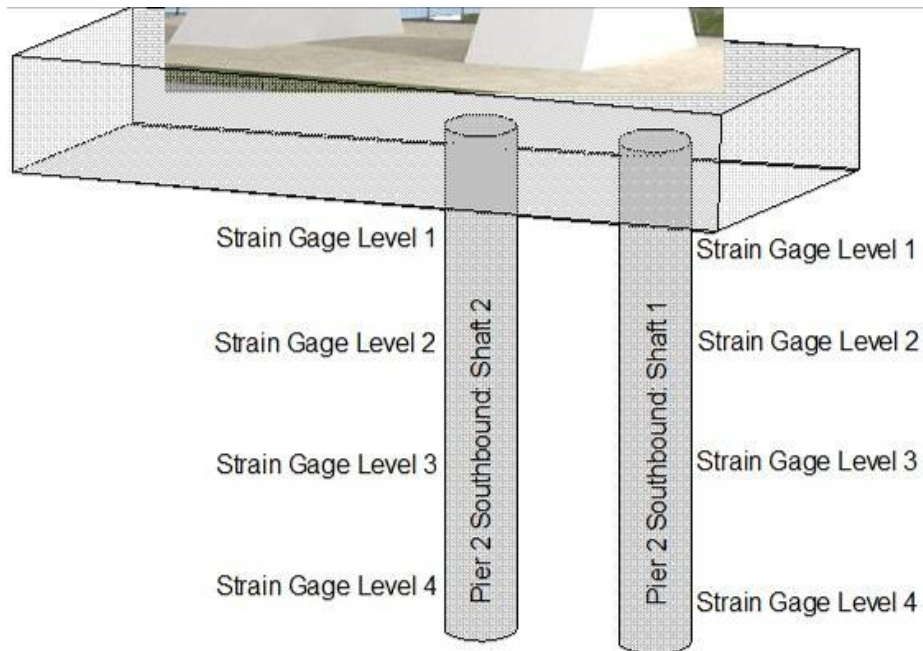
Figure 48. Illustration. I-35W bridge gauge levels on drilled shafts.

Figure 49. Photo. Cable bundles in reinforcement cage for I-35W bridge.

After the cages were fully instrumented, the excavations for the shafts were made. The shafts were drilled with two distinct sections. The top section was 7 ft (2.1 m) in diameter with a 0.50-inch (12.7-mm)-thick permanent steel casing surrounded by soil (see figure 50). The casing was necessary to keep the excavation clear. The casing ran approximately 3 ft (0.92 m) below the level of bedrock. The lower section was 6.5 ft (1.9 m) in diameter with no steel casing. GL2, GL3, and GL4 were located in this lower section of the shaft. After the excavation was created, the reinforcement cages were lifted and lowered into the excavation (see figure 51). After

reinforcement cage placement, the concrete for the shafts was poured with a single tremie. Upon removal of the tremie after concrete placement, a rebar instrumented with two additional TCs was inserted down the center of the shaft. The wires from all the TCs and strain gauges were run out through a 1.5-inch (38.1-mm)-diameter schedule 40 PVC conduit that was placed running out through the top of the shaft, underneath the future pier footing that would be constructed, and out to the DASs that were installed on site (see figure 52).

Figure 50. Photo. Top section of drilled shaft for I-35W bridge.
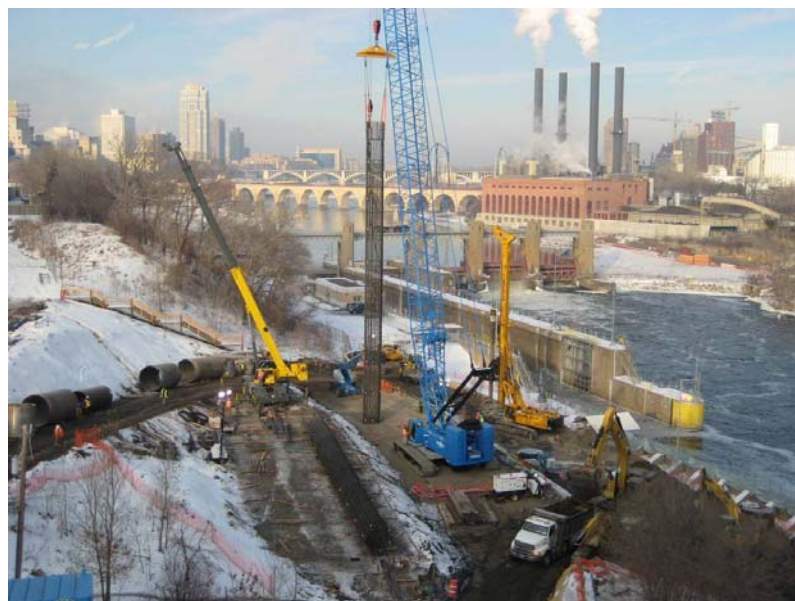
Figure 51. Photo. Placement of reinforcement cage for I-35W bridge shaft.

Figure 52. Photo. Conduits running from shafts to DAS boxes.

Two of the eight shafts were instrumented (see figure 52), and when all eight shafts were finished, time was alotted for the concrete to cure, the installation of the formwork, and reinforcement for the pier footing. The pier 2 footing was 81.02 ft (24.7 m) long by 34 ft (10.4 m) wide by 14 ft (4.8 m) tall (see figure 53) and was designed to support two columns (one for each concrete box girder section). It was reinforced with three layers of #18 bars at the bottom of the footing and three layers of #18 bars at the top. Along the top, W-shaped steel was used to support the reinforcing bars to prevent excess bending. TCs were installed at the base, the center, and the top of the footing. These TC wires were run out through a 2-inch (50.8-mm)-diameter schedule 40 PVC conduits down and out of the footing to the DAS boxes alongside the conduits from the shafts. The massive footing was equipped with PVC cooling tubes cast into the footing to help mitigate the mass concrete effects (see figure 54).

Figure 53. Photo. Lower layer of pier footing reinforcement for I-35W bridge.
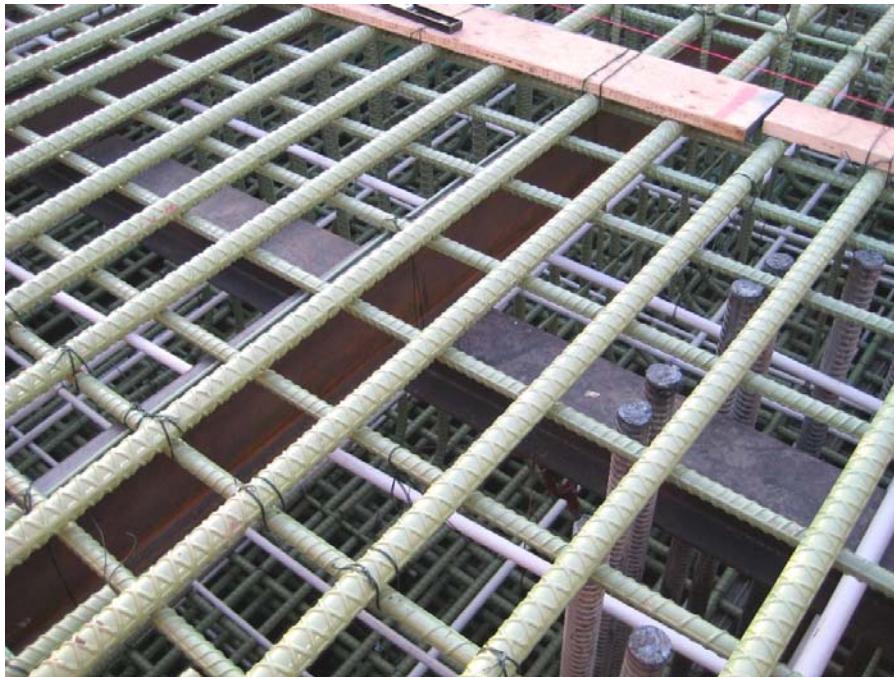
Figure 54. Photo. Upper layer of pier footing reinforcement for I-35W bridge.

Monitoring Setup and Procedure

For phase I of the study, the data collection was split into two subphases: the first phase consisted of the thermal monitoring of the shaft, and the second phase consisted of the thermal monitoring of the pier footing. The two phases were done similarly, and the setup for the thermal monitoring system was similar to the setup used in the voided shaft study discussed in chapter 3.

The system was made up of the following pieces: a Campbell Scientific, Inc.® CR1000 data logger, an AM25T 25-channel multiplexer, a Campbell Scientific, Inc.® Raven100 CDMA AirLink cellular modem, PS100 12-V power supply and 7-Ahr rechargeable battery, and a large environmental enclosure to protect all the materials from the elements (see figure 55). From the voided shaft study, it was discovered that a larger solar panel was needed to provide power to the system. As a result, a 35-W solar cell panel was utilized (see figure 56).

Figure 55. Photo. Thermal monitoring DAS for I-35W bridge shafts.

Figure 56. Photo. 35-W solar cell panel for I-35W bridge monitoring system.

The thermal monitoring procedure was identical to that of the voided shaft study. A thermal data sample was taken every 15 min and stored to the data logger at the same interval. Every hour, the Raven modem sent the collected data to the host computer at USF for data analysis. Once this data were received, they were automatically interpreted and plotted for use on the USF Geotechnical Research Web site. This thermal data from the shafts were collected from January 9 through January 21, 2008. At this time, the TC wires from the shaft were disconnected; however, the vibrating wire strain gauges (discussed in phase II) came with a thermistor. This thermistor was used to continue the thermal data from the shafts. The thermal data from the pier footing were collected from February 6 through February 25, 2008. No strain gauges were installed in the pier footing, so the only thermal data collected were stopped after this date. As with the voided shaft study, the battery voltage for the data logger was also monitored so that the logger did not lose power.

Along with the thermal monitoring setup, a CC640 camera was set up to take hourly photographs of the construction site (figure 57 and figure 58). (Note that the black bars in figure 57 are pointing to the camera.) It was powered by the same solar panel as the thermal monitoring system. The photos taken by the camera were sent back with the data collected from the TCs by the CR1000. The camera was useful for the thermal monitoring phase, but it was really installed as an aid in the construction load monitoring phase, which is discussed later.

Figure 57. Photo. CC640 jobsite camera with perspective outlines.

Figure 58. Photo. Sample camera shot from close-up camera on I-35W bridge.

System Results and Conclusions

The thermal monitoring procedure fared well. From the information gathered from the voided shaft study about the power consumption, the 35-W solar cell panel worked much better, and the battery voltage never dipped below 12V (see figure 59). Twice during the thermal monitoring phase, the system lost and then regained cellular communication with the host server. These occurrences seemed to correspond with the use of a large electric power plant directly adjacent

the system's cellular modem. This type of EMF is known to adversely affect such systems and is therefore a reasonable explanation. Other than these interferences, the thermal monitoring system worked as planned.
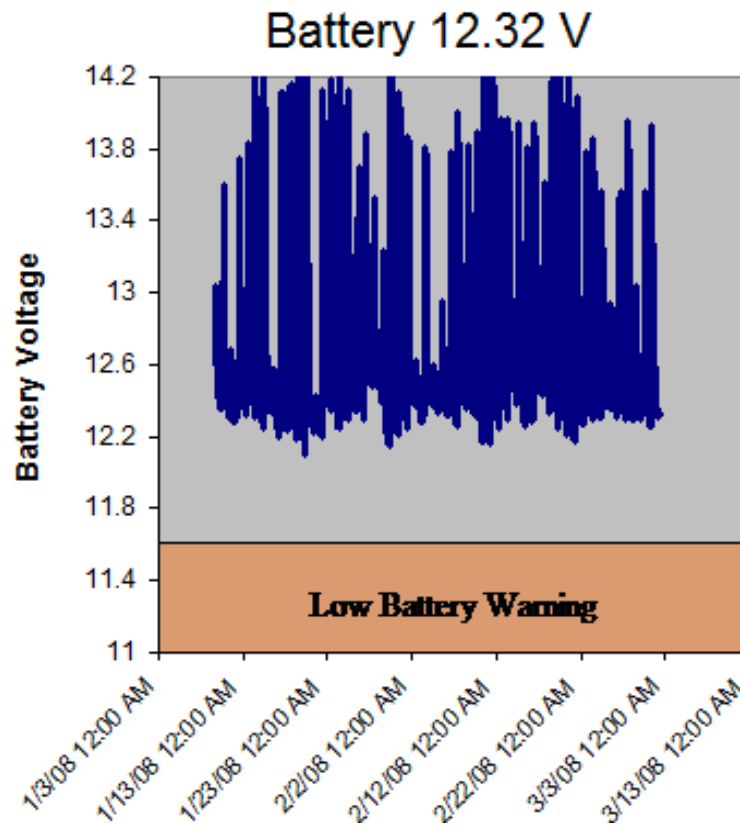

Figure 59. Graph. Data logger battery voltage from I-35W bridge monitoring system.

The concrete mix that was used was self-consolidating concrete that was designed to have a lower heat of hydration (see figure 60). Therefore, the temperature traces were expected to be lower than that of the voided shaft study. The thermal data from shaft 1 showed that the general average temperature attained in the concrete was 89.96 °F (32.2 °C) in the cage, and the two TCs at the core recorded higher temperatures of 125.96 °F (52.2 °C), which was a 36-°F (20-°C) difference (see °f = 1.8(°c) + 32

figure 61). Similarly, in shaft 2, the TCs mounted in the cage recorded an average temperature of 84.92 °F (29.4 °C), while the two TCs at the core recorded a higher temperature of 109.94 °F (43.3 °C), which was a 25-°F (13.9-°C) difference (see figure 62).

Subject: REQUEST FOR CONCRETE MIX DESIGN APPROVAL

Requested By: Kevin Heindel   Phone 651-686-4233
Firm Name: Cemstone Products Co.
Agency Engineer/Inspector Kevin Western (MnDOT)   SP # (I-35W Bridge)

Proposed Aggregate Sources

	CA #1	CA #2	CA #3	CA #4	Sand
Pit Number	82001	73006			82001
Pit Name	Grey Cloud	Martin Marietta			Grey Cloud
Nearest Town	Newport	St. Cloud			Newport
Size	3/8" (CA-80)	¾" (CA-50)			Sand
Sp.G. [1]	2.66	2.72			2.62
Absorption [1]	0.013	0.004			0.010

[1]Provided by Mn/DOT

Proposed Cementitious Sources

	Cement	Fly Ash	Slag
Manufacturer/Distributor	Lehigh	Headwaters	Holcim
Mill/Power Plant	Mason City, IA	Coal Creek, ND	Chicago, IL
Type/Class	Type I	Class F	Grade 100
Specific Gravity	3.15	2.55	2.89

Proposed Mix Designs

| Type of Work	Drilled Shafts		
Mix Number	ITF5035C		
Water (lbs/C.Y.)	270		
Cement (lbs/C.Y.)	242		
Fly Ash (lbs/C.Y.)	108		
Slag (lbs/C.Y.)	359		
W/CM Ratio	0.38		
Sand (Oven Dry, lbs/C.Y.)	1350		
CA #1 (Oven Dry, lbs/C.Y.)	410		
CA #2 (Oven Dry, lbs/C.Y.)	1280		
CA #3 (Oven Dry, lbs/C.Y.)			
CA #4 (Oven Dry, lbs/C.Y.)			
%Air Content	2.0		
Maximum Spread (3" Range)	20" to 23"		
VMA (oz/100 #CM) BASF-358	6.0		
HRWRA (oz/100 #CM) 7500	5.0		
AEA (oz/100 #CM) Daravair			

The above mixes are approved for use, contingent upon satisfactory site performance and continuous acceptability of all materials sources, by:

_____ _____ _____
Requested By   Date

_____ _____ _____
Mn/DOT Reviewer   Date

_____ _____ _____
Reviewed by: Mn/DOT Concrete Office   Date

Comments: Mix ITF5035C is for information purposes only and has been created by adjusting the aggregate proportions of mix ITF5035B so that the JMF may be met. No new JMF for mix ITF5035C has been created.

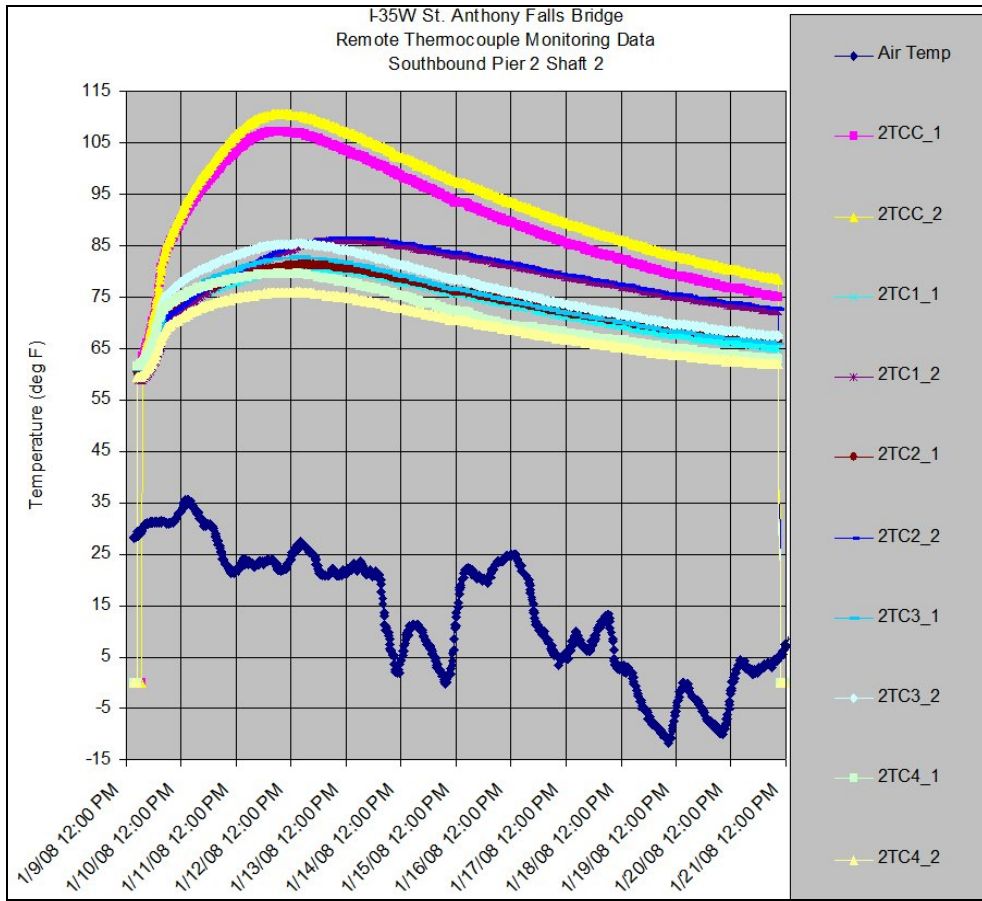| Written by: FMM	Revised by:	Approved by:
Date: 10.08.07	Date:	Date:

Figure 60. Diagram. Concrete mix design for drilled shafts on I-35W bridge.
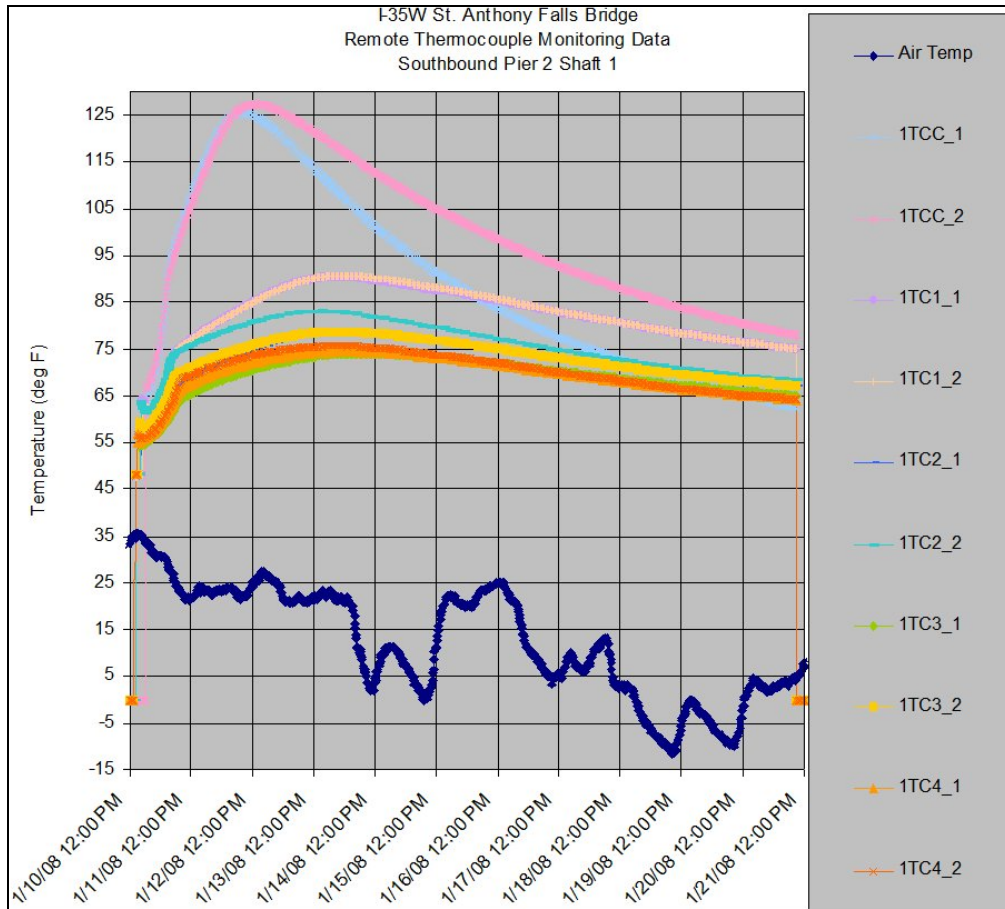
°F = 1.8(°C) + 32

Figure 61. Graph. I-35W bridge southbound pier 2 shaft 1 thermal data.

°F = 1.8(°C) + 32

Figure 62. Graph. I-35W bridge southbound pier 2 shaft 2 thermal data.

As discussed in the monitoring procedure, the TC wires from the shafts were cut on
January 21, 2008, and the thermal data were no longer collected. Upon connection of the
vibrating wire gauges from the shafts, the thermistors started to collect thermal data again. These
thermal data were analyzed and compiled with the data from the TCs, and the continuation of the
thermal curves were plotted (see figure 63 and figure 64).
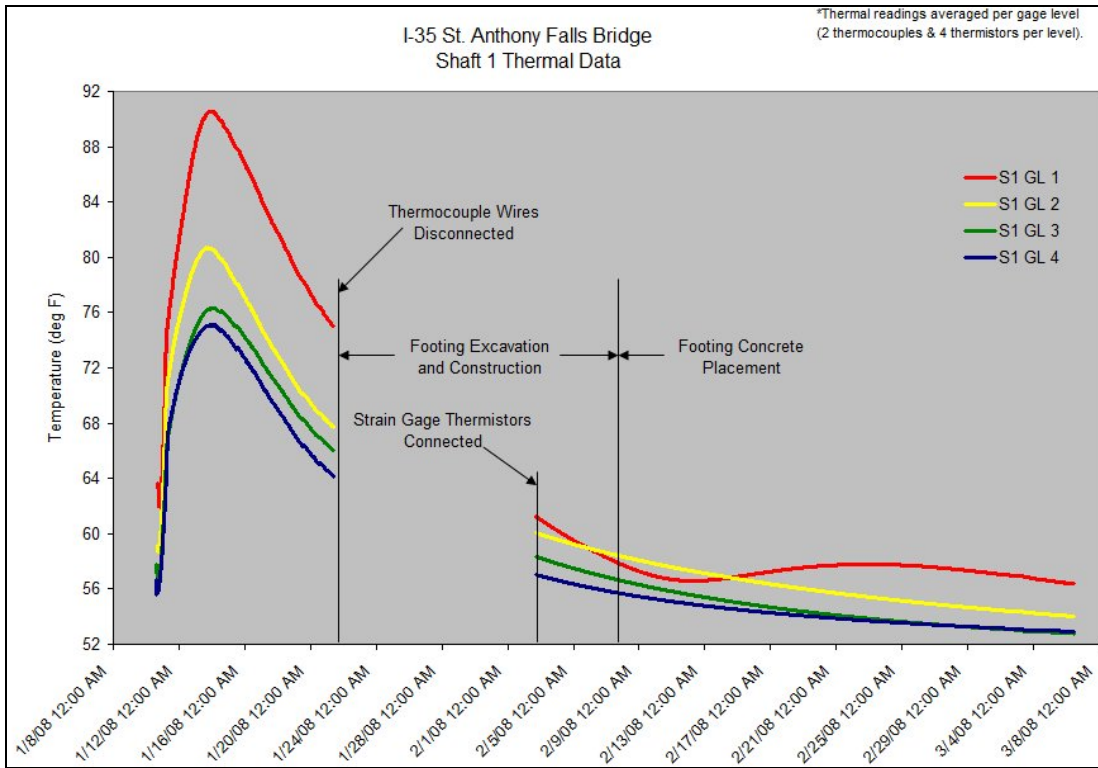
°F = 1.8(°C) + 32

Figure 63. Graph. I-35W bridge shaft 1 thermal data from TCs and thermistors.
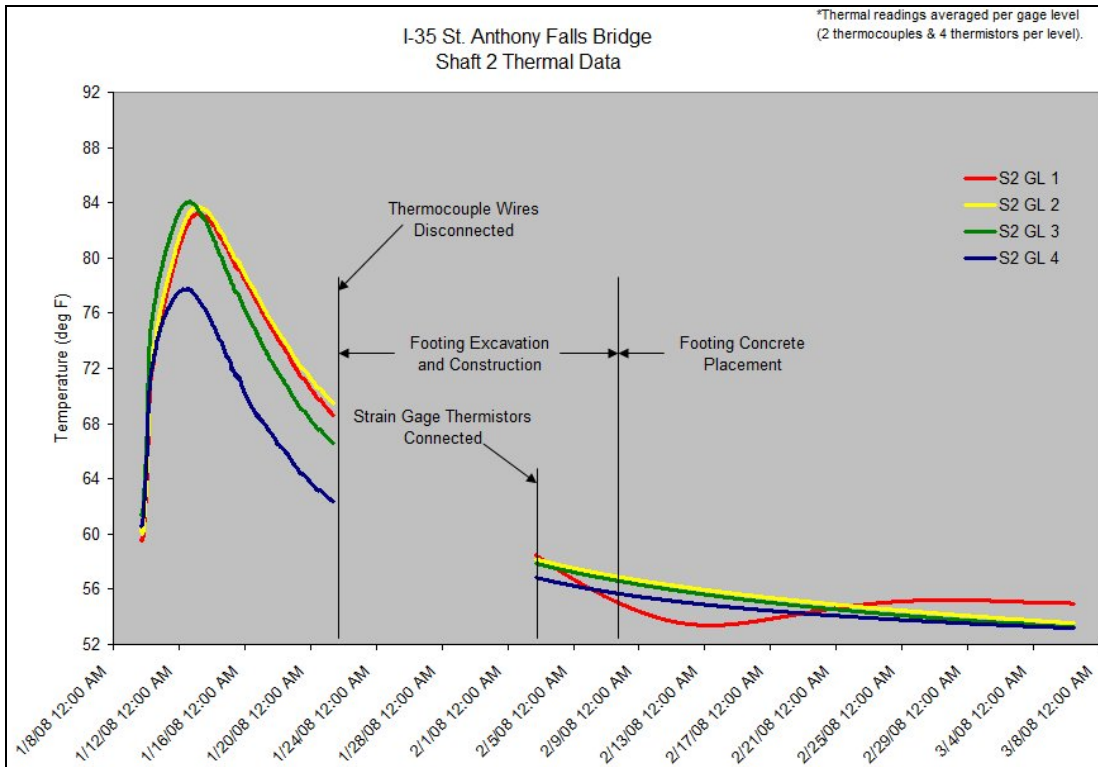
°F = 1.8(°C) + 32

Figure 64. Graph. I-35W bridge shaft 2 thermal data from TCs and thermistors.

53

As stated previously, the thermal data from the pier footing was collected from February 6 through February 25, 2008 (see °f = 1.8(°c) + 32

figure 65). As seen on the plot of the temperature over time, the TC in the extreme center of the footing recorded a maximum temperature of approximately
140 °F (60 °C), while the TC at the center bottom of the footing only reached a temperature of approximately 90 °F (32.2 °C). The same concrete mix was used throughout the pier footing, so it should all have been roughly the same temperature; however, the ambient temperature, which ranged from 40 to -10 °F (4.4 to -23.3 °C), caused the temperatures to drop drastically closer to the outside edges of the footing.
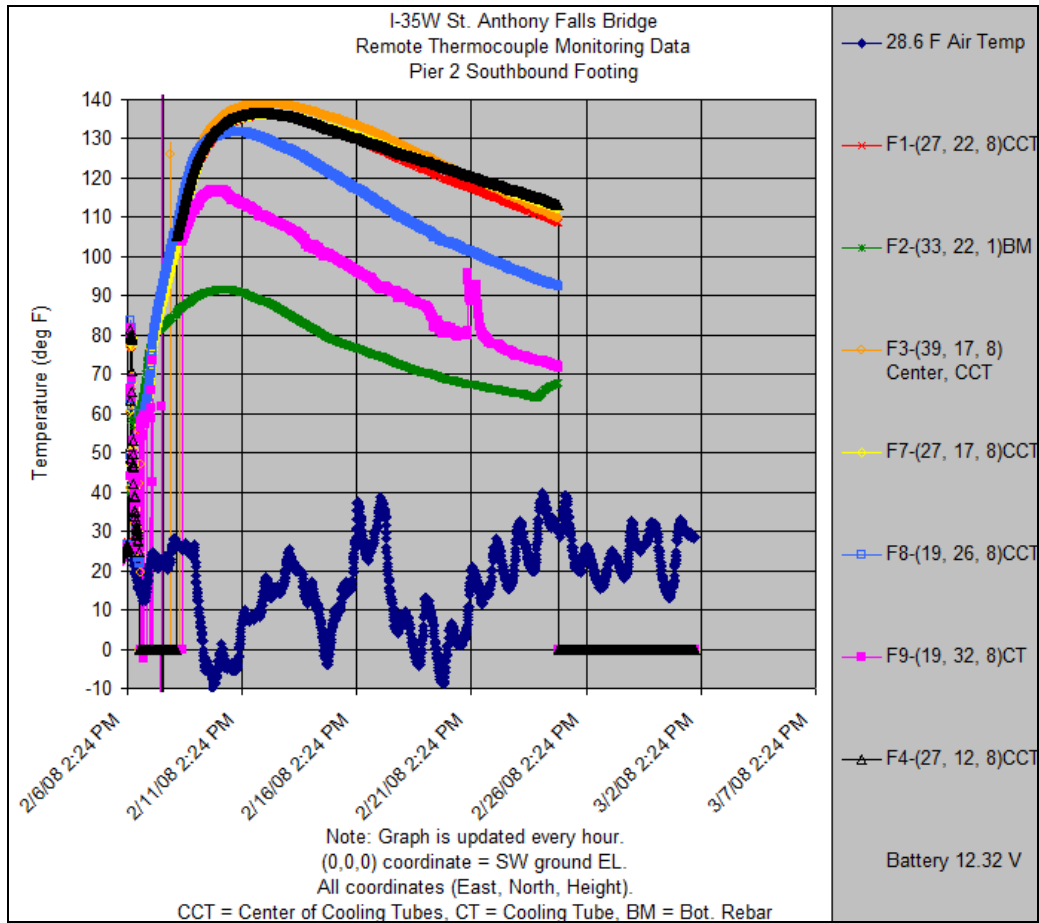
°F = 1.8(°C) + 32

Figure 65. Graph. Pier 2 southbound footing thermal data from TCs.

PHASE II—CONSTRUCTION LOAD MONITORING

This phase of the study expands from the voided shaft study. In phase II, the loads placed on the shafts by the pier footing, columns, and segments of the superstructure were monitored. As shown in figure 46, this phase actually began at the start of the footing construction, but no data were expected until the shaft cured and the footing concrete was poured.

For the section on construction and instrumentation, there was obviously an overlap with the construction sequence. Therefore, this section of the report does not go into detail about the construction of the drilled shafts nor of the pier footing. However, more emphasis is placed on the strain gauges that were installed in the drilled shafts. For the pier columns, however, the construction and instrumentation is explained. Focus is provided to the construction phases of the column and how it affected the construction loads placed on the drilled shafts.

Construction and Instrumentation

The strain gauges used in this study were provided by Geokon, Inc.™. They were model 4911 "sister bars" and were specifically made for ease of installation (see 1 inch = 25.4 mm

figure 66). They came with the strain gauge preinstalled on a 54.25-inch (1,377.95-mm) length of #4 bar. This bar was then tied to the existing reinforcement in the shaft or column. Since the gauge was on a #4 bar, it did not provide enough extra steel area that the cross section of the element was altered (providing the element was quite large). Therefore, it only minimally affected the calculations of converting strain to load. The strain gauges in the shafts were installed at the same four levels as the TCs: GL1, GL2, GL3, and GL4 (see figure 48). However, two types of strain gauges were used. At each level, 4 vibrating wire (VW) strain gauges and 2 resistance (RT) strain gauges were installed, which made for a total of 16 VW gauges and 8 RT gauges per shaft. The VW gauges were installed at a 90-degree separation (see figure 67), with the RT gauges at 180-degree separation coupled with the VW gauges (see figure 68). The VW gauges, as explained in phase I, came equipped with a thermistor. These gauges were not capable of recording strains at high rates (for dynamic measurements), which was why RT gauges were also installed.
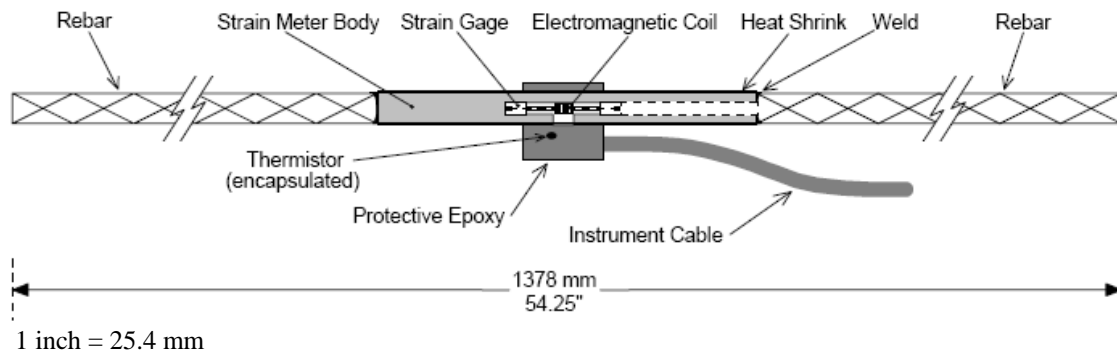

1 inch = 25.4 mm

Figure 66. Illustration. Detail of Geokon, Inc.TM 4911 sister bar strain gauges.

Figure 67. Photo. VW gauge installed in shaft reinforcement cage.

Figure 68. Photo. Coupled VW (blue cable) and RT (green cable) gauges.

At each main pier, two reinforced concrete columns sat on top of the footing to support the superstructure for one direction of traffic. The columns were constructed with a varying cross section (see figure 45). The critical cross section was at the midheight of the columns where the strain gauges were placed. The columns were cast in three separate pours.

First, the longitudinal bars running up through the columns were spliced to the longitudinal bars embedded in the pier footing (see figure 69). Then, the formwork for the lower half of the column was set in place. The first pour was a small 200-yd^3 (182.8-m^3) pour to get the column started. After that, the horizontal reinforcement was set inside the formwork up to the midheight

of the column. After the horizontal steel was in place, the next level of longitudinal steel was spliced to the first level so that the bottom of the bars were embedded in the lower half of the column. After the reinforcement up to midheight was installed, the second pour occurred. This second pour placed the concrete up to midheight of the column (see figure 70). During the next phase of construction, the formwork for the top half of the column was placed, and the horizontal steel in the column was installed. The column midheight strain gauge installation also took place at this time. The critical section of the column was 8 by 16 ft (2.44 by 4.88 m) with reinforcement that consisted of 44 #20 bars (see figure 71).

Figure 69. Photo. Reinforcement for first column pour for I-35W bridge columns.

Figure 70. Photo. Reinforcement at midsection of columns for I-35W bridge.
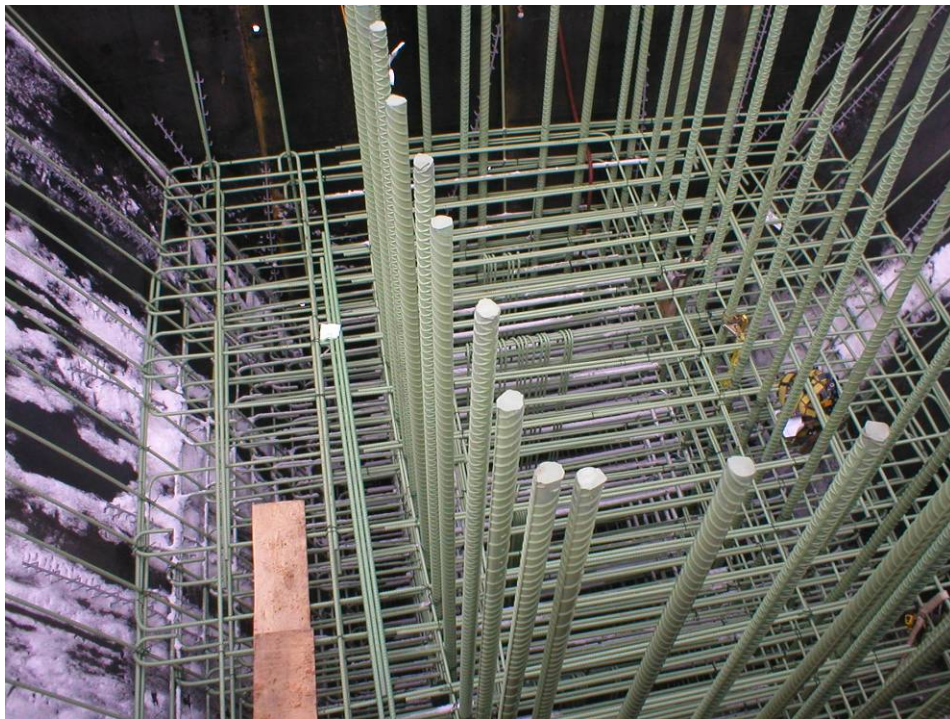

Figure 71. Photo. Longitudinal and horizontal column reinforcement.

The total instrumentation for each column consisted of four vibrating wire strain gauges and four resistance-type strain gauges. The same coupled gauges that were installed in the shafts were used in the columns (one VW gauge and one RT gauge per sister bar). One sister bar unit was installed at each corner of the column in the critical section (see figure 72). By placing the gauges in the corners of the cross section, the strain at the extreme fiber of the column could be

measured. Once the gauge installation units were tied and secured in place (see figure 73), the wires were run out of the top of the column formwork so that the cables could be bundled together. Then, the wires were brought back down to the midsection of the column and were run out through the 2-inch (50.8-mm) schedule 40 PVC conduit that extended up to the midheight of the columns (see figure 74). The wires ran through the conduit, down the column and shaft cap, and out to the temporary DAS that was installed on site. In addition to these strain gauges, the University of Minnesota Department of Civil Engineering also placed five strain gauges in each column that was installed in the same locations as those done by the FHWA team, but with an additional gauge located in the center of the column. The wires for these gauges were bundled with the wires from the FHWA gauges and pulled out to the DAS at the same time. These cables were grey (as opposed to blue and green used by FHWA) and can be seen clearly in figure 74. No presentation or analysis of the University of Minnesota gauges is presented herein.
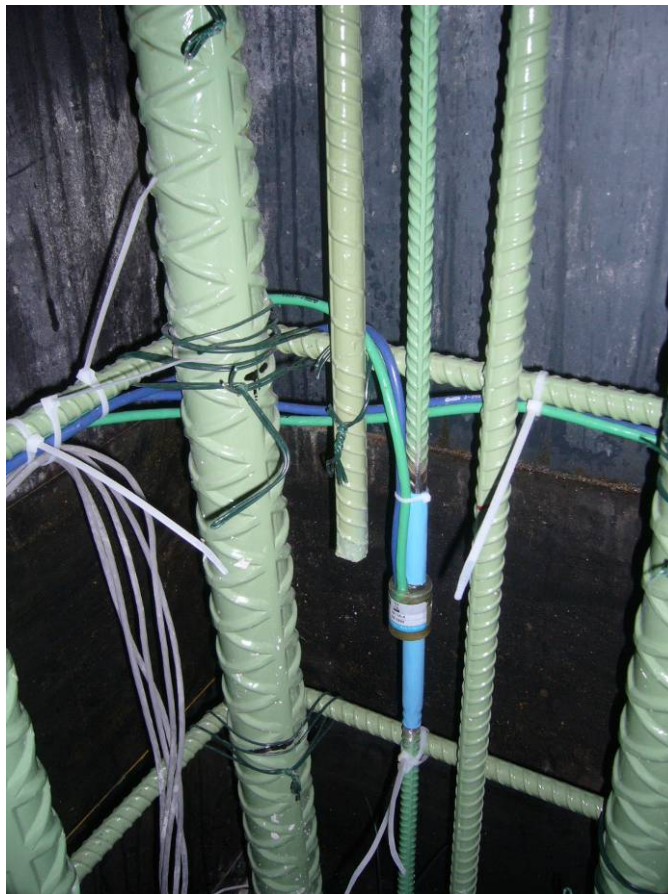

Figure 72. Photo. Coupled gauge installed in corner of column of I-35W bridge.

Figure 73. Photo. Gauge wires tied and secured in column of I-35W bridge.

Figure 74. Photo. Wires exiting through conduit.

Monitoring Setup and Procedure

For phase II of the study, the data collection was split into two subphases: the load monitoring of the shaft and the load monitoring of the columns. The reason for this split was that a large amount of dead load on the shaft came from the construction of the pier footing and the columns. Furthermore, if the loads on the shafts were monitored first, checking that the measured loads

were correct was much easier because the load was simply the dead load of the footing and columns. Each phase of monitoring was carried out in the same way. The monitoring setup and procedure is explained through a discussion of the three different systems that were installed and used during this phase of the study.

System 1 was the same thermal monitoring system that was used in phase I of the study as well as the voided shaft study discussed in chapter 3. It was reused during this phase of the study as the monitoring and transmission system for the CC640 field camera. The camera was set up to take a picture every hour and then transmit that picture back to the host computer via the cellular modem. During the thermal monitoring phase of the study, system 1 was powered by the installed solar cell panel with a backup deep cycle battery. During phase II, the system was moved to alternating current (A/C) power, but a deep cycle battery was kept in reserve in case the A/C power was disrupted. This A/C power was provided by the U.S. Army Corps of Engineers who had an A/C power source adjacent the site.

The second and third systems were installed at almost the same time, but they had different capabilities and assignments. System 2 was designated to collect data from the vibrating wire gauges installed in shafts 1 and 2 as well as those in the interior and exterior columns. This system also recorded the gauge temperatures via changes in thermistor resistance. A total of 50 vibrating wire gauges and 50 thermistors were connected to this logger via two AVW200 two-channel spectrum analyzers. Each channel of the AVW200 units was connected to a low-power multiplexer (MUX) 16/32B (four in all). MUX 1 was connected to shaft 2 (16 gauges), MUX 2 was connected to shaft 1 (16 gauges), MUX 3 was connected to the interior column (10 gauges), and MUX 4 was connected to the exterior column (10 gauges) (see figure 75). The true value of the AVW200 data was unused because many pieces of data quality were recorded along with the raw strain and temperature values of interest. These additional measures of data quality (e.g., signal-to-noise ratio, etc., four total) were intended to provide insight into the health of the gauge and triple the required storage space and to significantly reduce the overall duration of monitoring without remote collection from the circular data buffer. At the rate of storage, the number of channels monitored, and amount of on-board memory, only a 2-week period could be stored before circular overwrite. However, with hourly collections, this was never a problem.

Figure 75. Photo. Wire connection to system 2.

The system monitoring the VW gauges (system 2) used a Campbell Scientific, Inc.® CR1000 data logger, while the system monitoring the RT gauges (system 3) used a Campbell Scientific, Inc.® CR9000 data logger. System 2 worked similarly to the thermal monitoring system. A sample was taken and stored to the data logger every 15 min. Every hour, this stored information was sent back to the host computer at USF to be compiled and analyzed. System 3 took a sample at a rate of 100 Hz (100 samples per second). However, all of the data were not stored. Rather, the mean, maximum, and minimum of these samples were stored every 15 min. Then, every hour, the stored data points were sent back to the host computer similar to the data from system 2. This provided the user with a better idea of the strain in the system because of the high sampling rate. However, this method used a large amount of power. The monitoring system sampling and storage rates and other information are provided in table 2. Due to differences in the two DAS board configurations, each system had a dedicated Campbell Scientific, Inc.® Raven100 CDMA AirLink cellular modem. Three large environmental enclosures were used to house and protect the DAS units and wire connections from the elements (see figure 76).

Table 2. Summary of monitoring systems for I-35W bridge monitoring study.

System Parameter	System 1	System 2	System 3
Gauge type	TCs	VW strain gauges thermistors	RT strain gauges
Data logger	CR1000	CR1000	CR9000
Sampling rate	15 min	15 min	100 Hz
Storage rate	15 min	15 min	15 min (sample mean, sample max, and standard deviation)
Transmit rate	1 h	1 h	1 h

Figure 76. Photo. Construction load monitoring systems (VW = blue (right) and RT = green (left)).

For this phase, it was known that a large amount of power would be consumed by the monitoring systems. Therefore, it was necessary to provide the systems with enough backup power to prevent power problems similar to the voided shaft study. Each system was integrated with a deep cell battery that provided power in case of a power failure (see figure 76). However, there was a problem with this system; the PS100 12-V power supply that recharges the 7-Ahr battery could only receive power from either an A/C source or the solar panel but not both. Therefore, a battery manager was installed to bypass this limitation.

As with the thermal data from the shafts, once these data were received and reviewed, researchers plotted the data online at http://geotech.eng.usf.edu/I35.html. The strain in the shafts at the four different levels was monitored beginning on February 6, 2008, with the pier footing concrete placement. The strain data from the shafts were computed into construction loads, and an annotated graph was updated online (see 1 kip = 454 kg
1 yd = 0.914 m
1 ft = 0.305 m

figure 77). Along with this graph, pictures from these events were captured using the CC640 field camera, and they could be related to the points of interest on the graph. This aided in verifying the loading event and the amount of load that was calculated in the shaft (see figure 78 through figure 81).
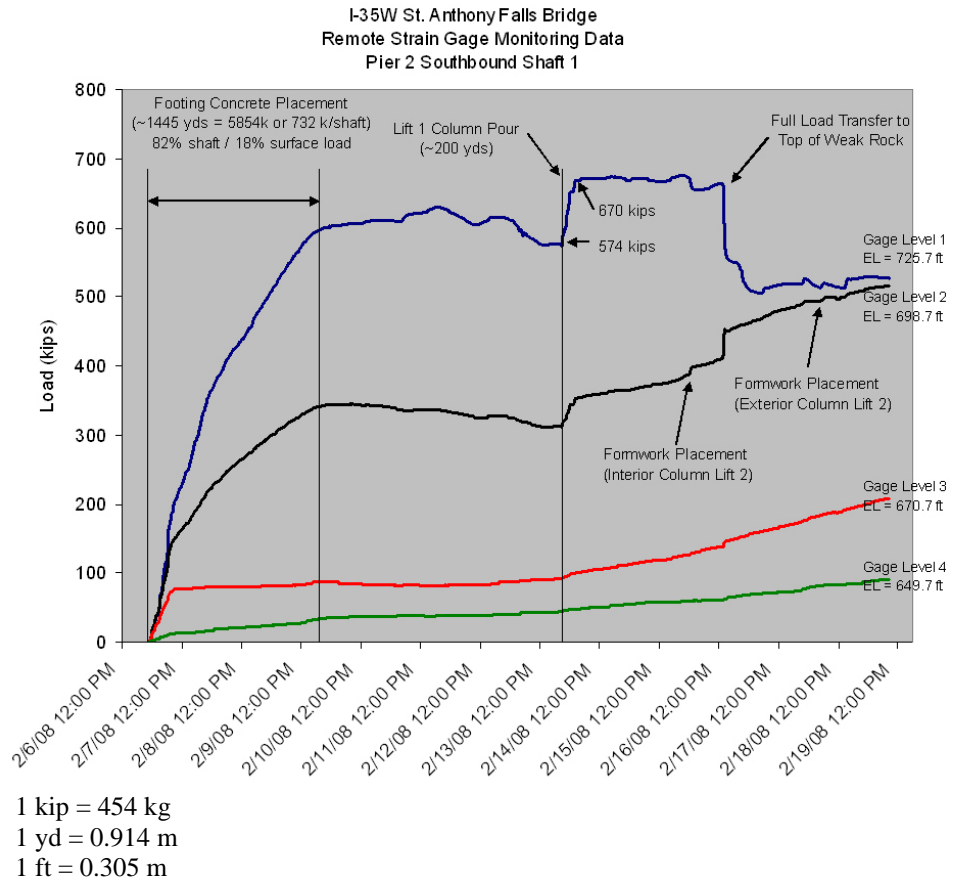
Figure 77. Graph. Shaft construction loads and events.

1 kip = 454 kg
1 yd = 0.914 m
1 ft = 0.305 m

Figure 78. Photo. Pier footing concrete placement.

Figure 79. Photo. Lift 1 column concrete placement.

Figure 80. Photo. Interior column lift 2 formwork placement.

Figure 81. Photo. Exterior column lift 2 formwork placement.

As seen in figure 81, the column foundation became too large to view in its entirety by the close-up camera location. Therefore, the CC640 field camera was moved to a new location on top of the University of Minnesota BOBMAIN building on the southwest bank of the river. This new position afforded oversight of the entire project from end bent to end bent and was used to dovetail recorded strains to construction events (see figure 82).

Figure 82. Photo. New perspective from CC640 field camera.

System Performance

The three monitoring systems used during the construction load monitoring phase fared well. System 1 lost and then regained communication with the host server twice. These occurrences seemed to correspond with the use of a large electric power plant directly adjacent the system's cellular modem. This type of EMF was known to adversely affect such systems and was therefore a reasonable explanation. As stated in the monitoring procedure, system 1 was repositioned in early March 2008. This system worked without issues from March 5, 2008, to March 19, 2008, when communication between the camera and logger failed. Review of the system revealed the camera was still recording images to its internal compact flash card, but images were not transferred to the logger for scheduled collection. Subsequent baud rate reduction cleared the problem.

As stated in the monitoring procedure, power consumption was a large concern for this phase of monitoring. The power of system 1 was stable throughout this phase. The system was originally completely powered by solar energy, and a deep cycle battery was used as a backup. In early March 2008, the power source was switched to constant A/C (with battery backup) and provided the system with more stabile voltage (see figure 83). At no time did the voltage approach the critical logger shutdown voltage. Results of both the close-up pictures and the overview pictures are shown in figure 78 through figure 82.
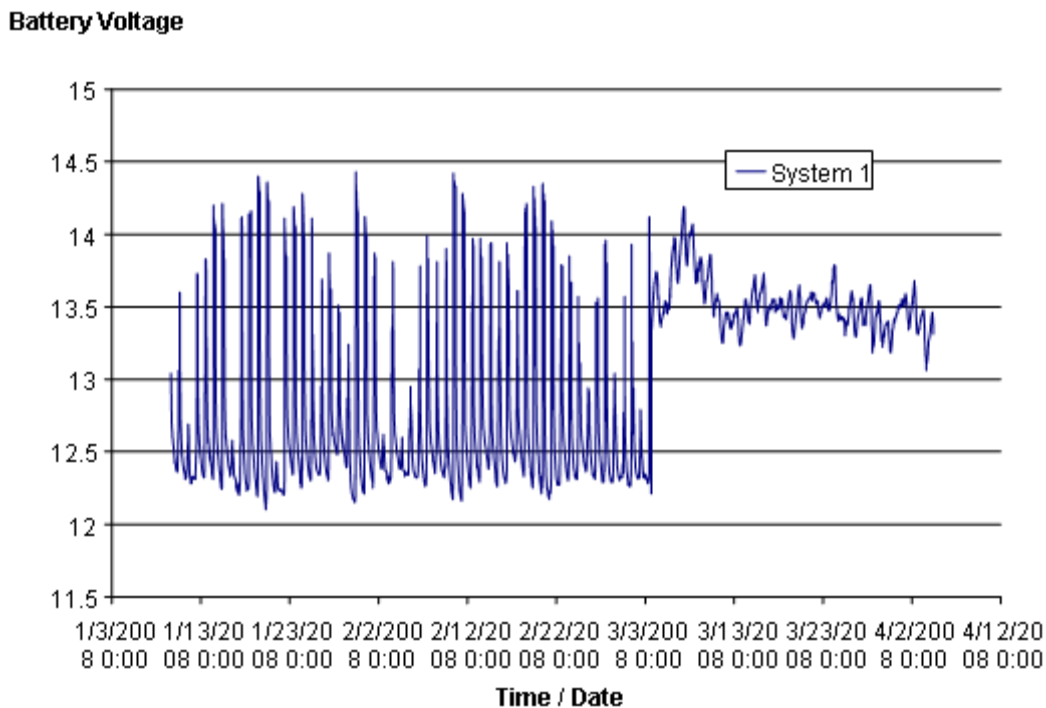

Figure 83. Graph. System 1 battery voltage over time.

The results of system 2 were a little less desirable. The cellular communication with this system became somewhat of a concern with regards to reliability. This system, which was similar to system 1, logged data that were collected without issue from February 5 through March 26, 2008. For a short period following this time frame, no collections were possible. It was unclear

67

whether the system was still powered and logging; however, up until the last collection, the power cycles were regular (see figure 84). Since the critical threshold voltage of 11.2V was not approached at any time, it was unlikely that power interruption was the cause of the communication errors. The concern with the intermittent communication was resolved, but the data collected from one of the four multiplexing units responsible for monitoring nine of the vibrating wire gauges were unintelligible. An onsite visit was required to find a partially cut wire between the MUX unit and AVW-200, and it had started as intermittent and ultimately resulted in complete failure. Simple repair of this connection resumed full operation; data from this time period were not obtained from those gauges.
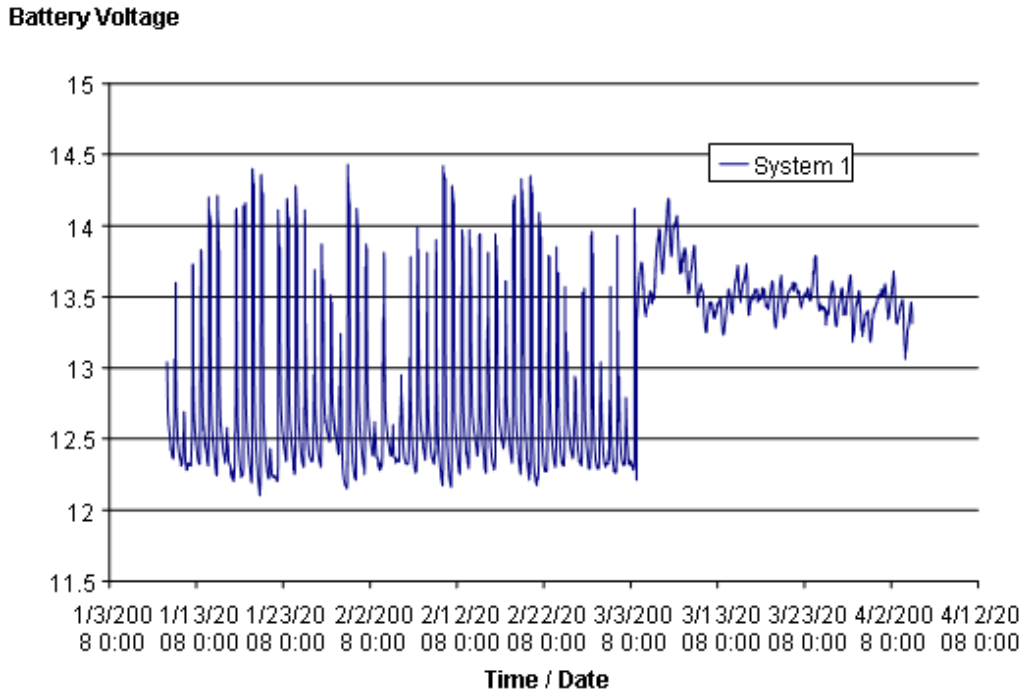

Figure 84. Graph. System 2 battery voltage over time.

The results of system 3 were better than those of system 2 because communication never faltered. The primary difference between this system and the other two was the logger type, CR9000 versus CR1000, the latter of which had not been consistent. The battery voltage of system 3 varied less than the battery voltage of system 2, yet neither system exhibited a power disruption (see figure 85).
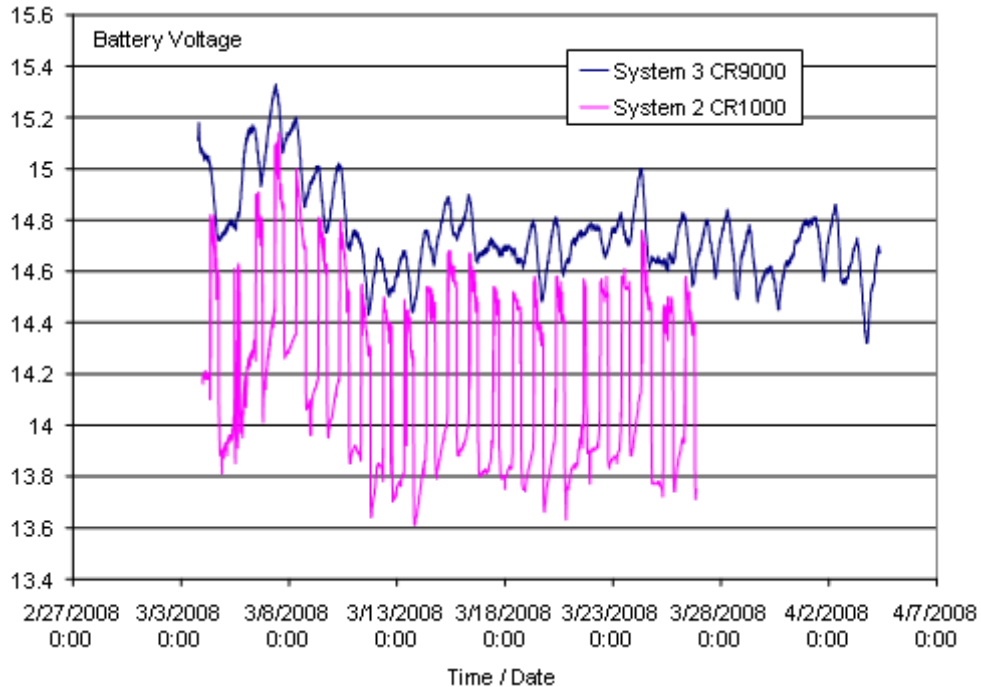
Figure 85. Graph. System 2 versus system 3 battery voltage.

Once a sufficient amount of data were collected, the host Web site for the data review was modified to include hover points associated with pathways to videos or data locations (see figure 86). The link to the south camera perspective takes the user to a page that shows a video made of time lapse photos taken by the CC640 field camera in its altered position atop the University of Minnesota building. The link to the west camera allows users to navigate to a page that shows a video made of time lapse photos taken from the Web camera set up by MnDOT. The pier 2 close-up camera link shows a video made of time lapse photos taken by the CC640 field camera in its original close-up position. All of these videos provide a quick look at the construction progress of the bridge from different vantage points and were used to relate the strain data to specific construction events. The FHWA SSHM site link (http://geotech. eng.usf.edu/I35.html) takes users to a separate page with a close-up view of the site with more hover points (see figure 87). Each link takes users to a plot of the strain of that subject over time (see figure 88 through figure 91). These graphs were broken down into daily increments as shown by the dotted lines running vertically on the graphs. The spaces between these dotted lines are links that take users to the pages with the Web cameras showing the construction progress up to that date. This way, the strain data can be more accurately related to construction events. Negative values on the graphs indicate compression.
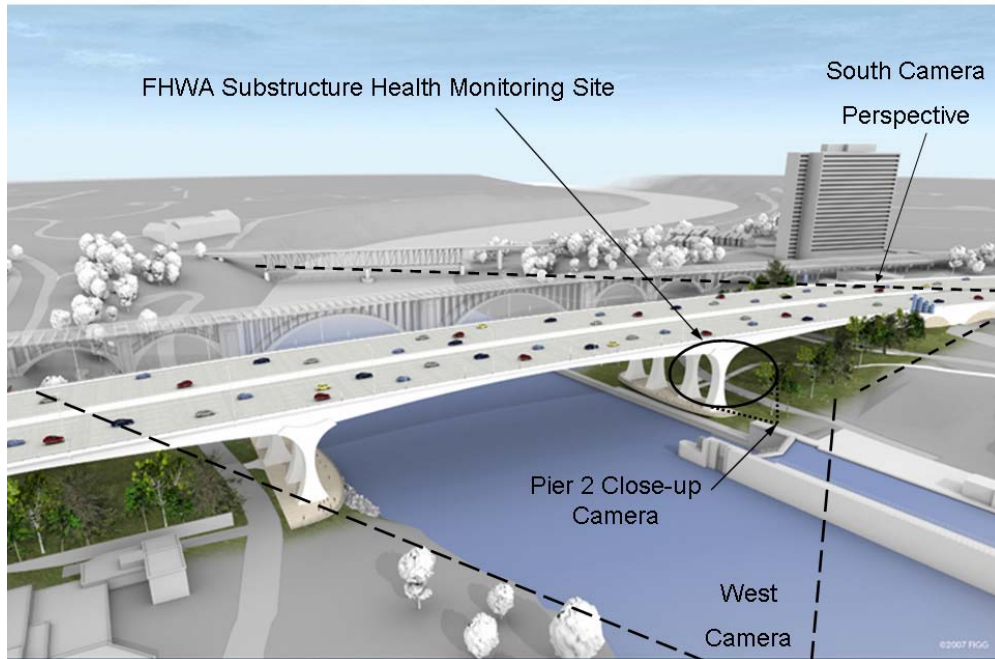
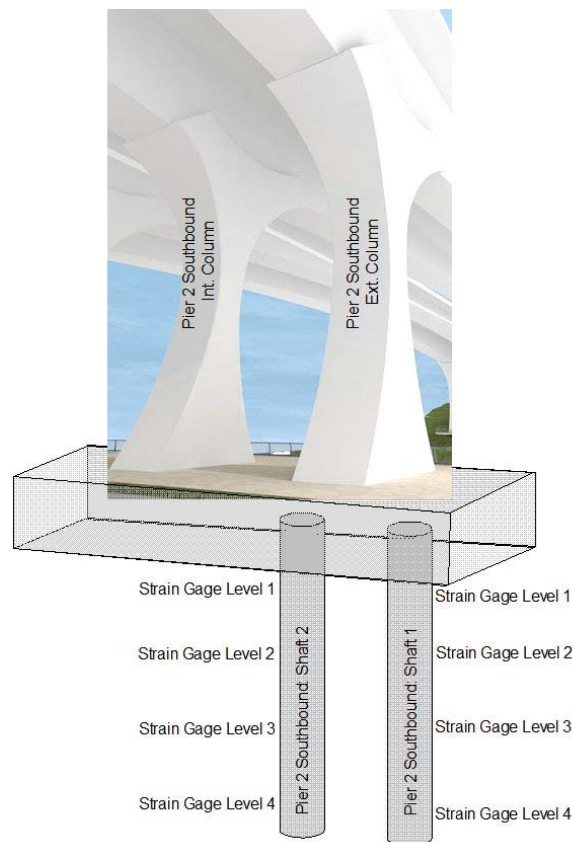**Figure 86. Illustration. Hover points on the main page of St. Anthony Falls Bridge health monitoring Web site.[9]**

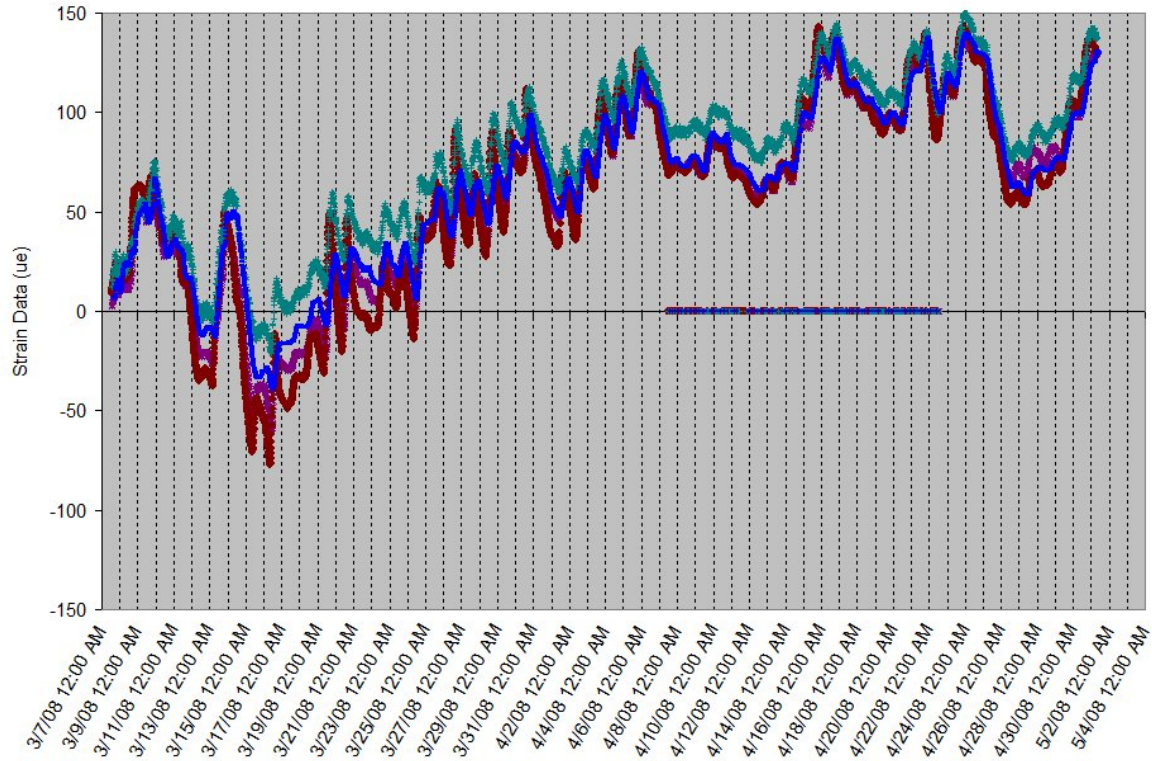**Figure 87. Illustration. Instrumentation scheme for the St. Anthony Falls Bridge health monitoring project.**
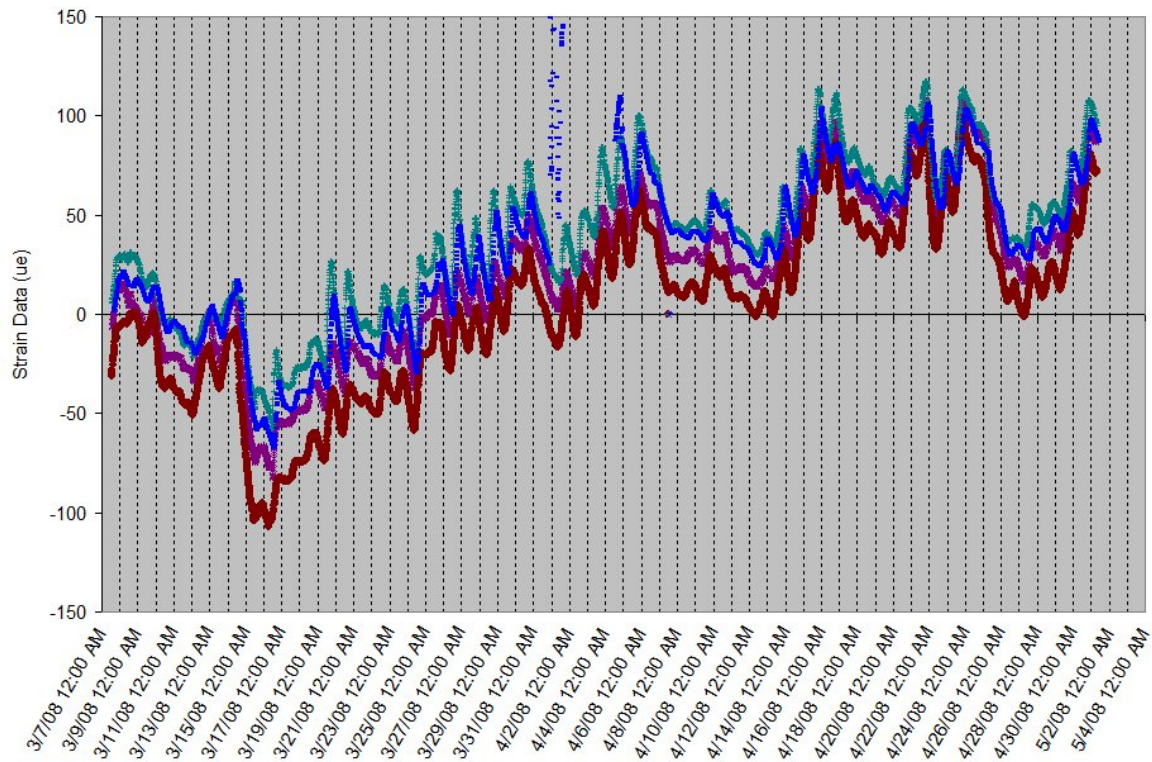
Figure 88. Graph. Pier 2 interior column strain.

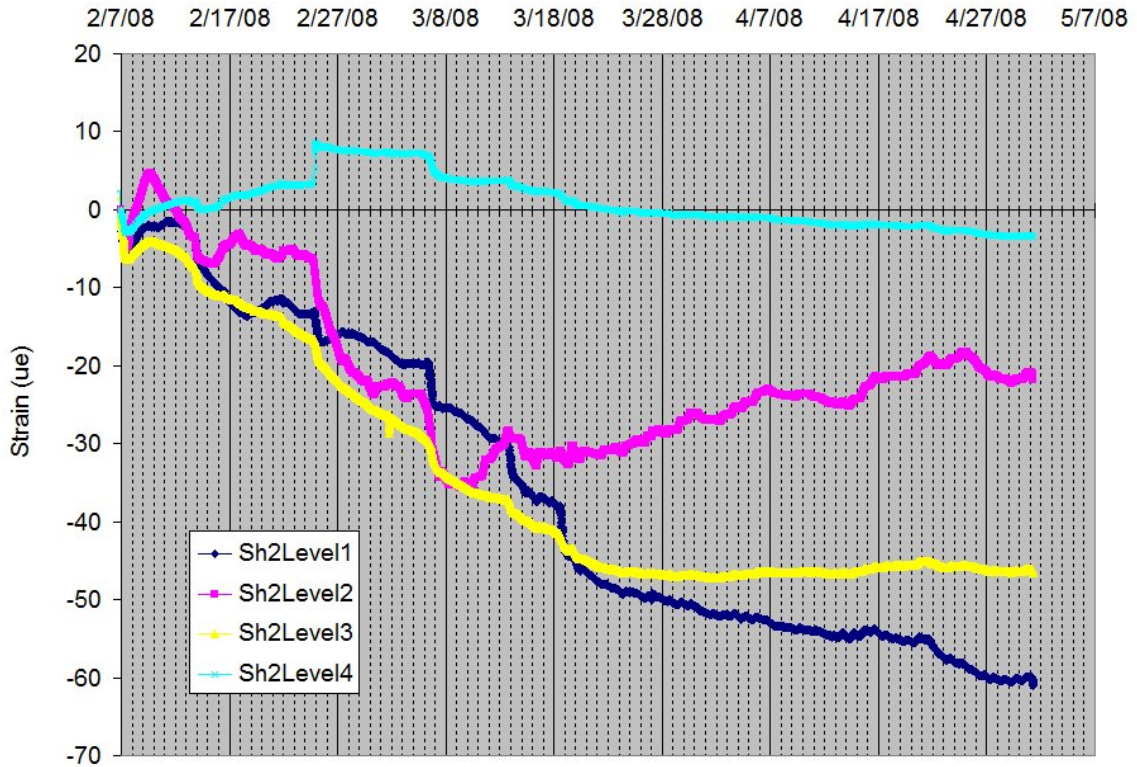**Figure 89. Graph. Pier 2 exterior column strain.**

71

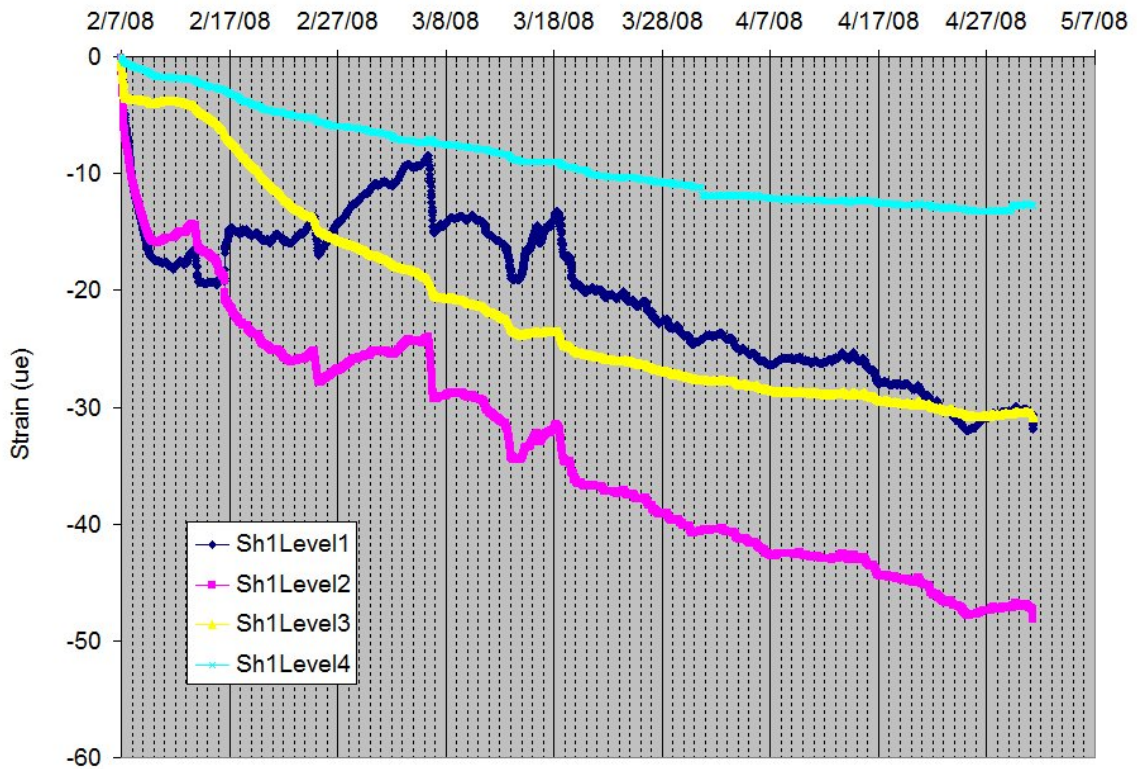**Figure 90. Graph. Pier 2 shaft 2 all levels strain.**

Figure 91. Graph. Pier 2 shaft 1 all levels strain.

The load on pier 2 was somewhat complicated by indeterminate reactions from false work used to support the cast-in-place span 1 box girders (from end bent 1 to pier 2). As a result, the total load from span 1 was not felt by pier 2 until the bridge was almost completed and as the false work was removed. Precast box girder sections (timeline indicated in figure 92 and figure 93) were installed almost daily, extending from pier 2 toward pier 3 and cantilevered out over the Mississippi River. However, by correlating the number of box sections and their respective weights to the measured strain in each column, the column strain gauges were calibrated with increased confidence. Figure 94 shows the computed load from strain, concrete modulus, area as a function of the logging, and the theoretical reaction due to the known concrete box girder weights using lever arm.
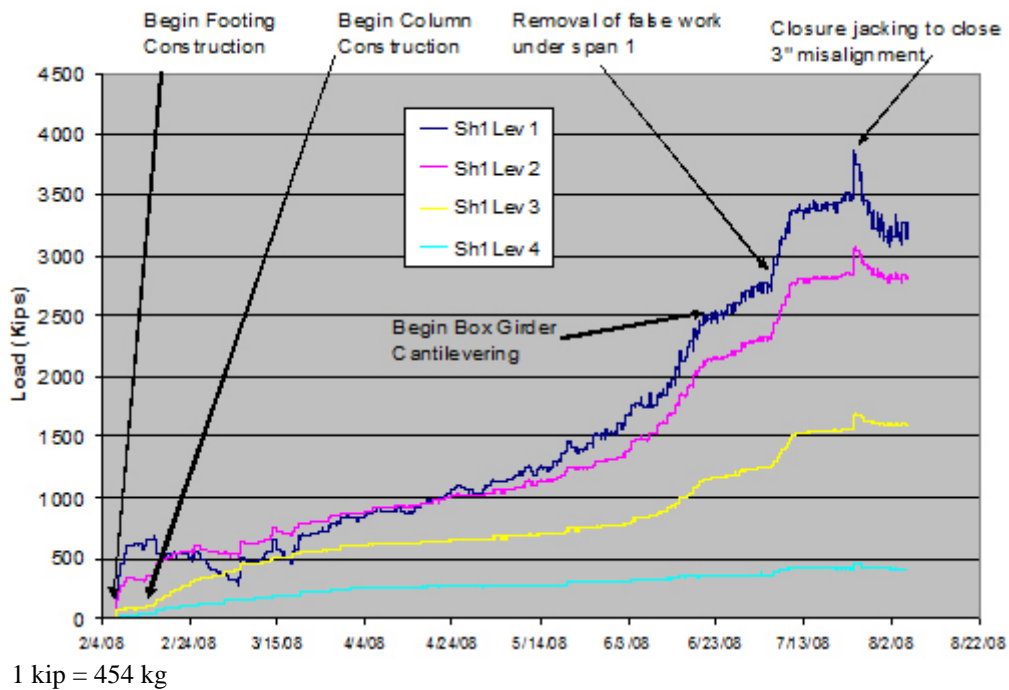

1 kip = 454 kg

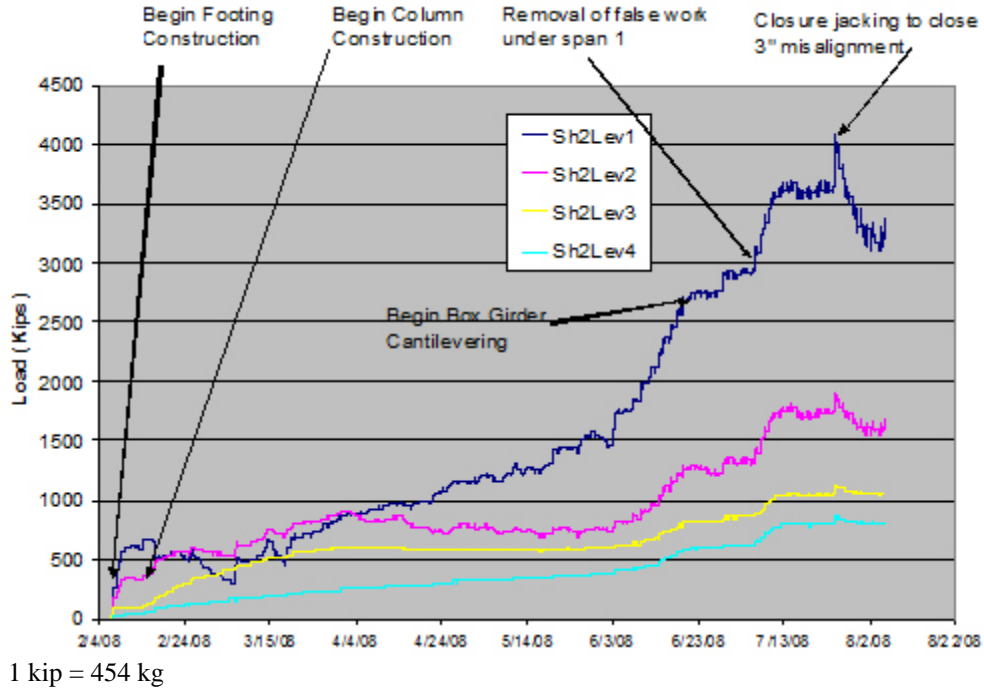**Figure 92. Graph. Shaft 1 loads throughout the entire construction sequence.**

1 kip = 454 kg

Figure 93. Graph. Shaft 2 loads throughout the entire construction sequence.
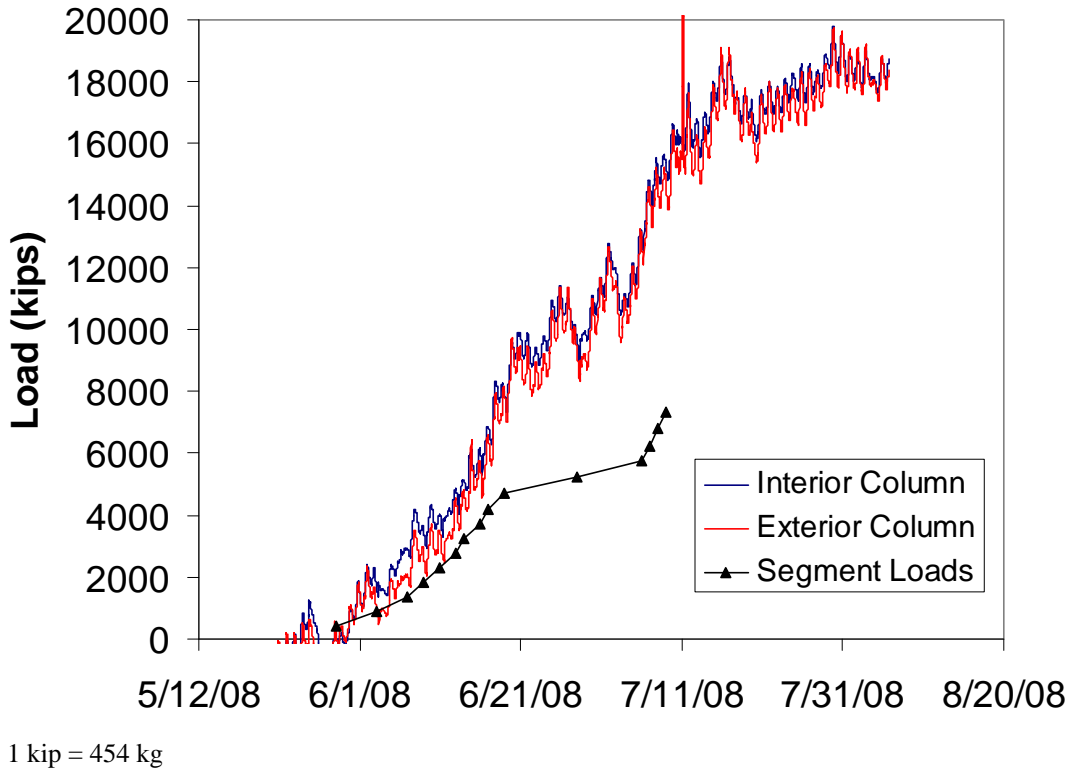

1 kip = 454 kg

Figure 94. Graph. Column loads compared with segment placement.

74

Unlike the shaft gauges located beneath the footing, column loads were subject to daily temperature fluctuations, which can be seen in figure 94. Additionally, the stark difference between the calculated segment load effects on the overall column load was caused by relaxation of the false work support as the cantilevering load provided uplift throughout span 1.

Construction Phase Monitoring Completion

Recall that only two shafts out of the eight in pier 2 (southbound) were instrumented; both were on the south edge of the footing, providing similar responses to the construction loads when considering column bending effects. Unfortunately, the load carried by the other six shafts was not monitored, and the response therein could only be estimated based on engineering principles. Figure 92 and figure 93 show the loads (as converted from measured strains, positive compression) detected in shafts 1 and 2. These figures are annotated to show several significant points in the construction sequence that help explain changes in the load versus time relationship.

By looking at both the shaft response and the column strains, a clearer picture of the loading can be obtained. Figure 95 and figure 96 show the strains recorded for both the interior and exterior columns found on the same eight shafts beneath pier 2 southbound. The increased compressive loads (positive sign) shown in shafts 1 and 2 correspond to expansion required to obtain the necessary tolerances followed by jacking closure at the center span misalignment. This is shown by the increased compression strain on the south edge of the columns that correspond to decreased compression strain (of similar magnitude) on the north edges followed by a reversal upon closure jacking.
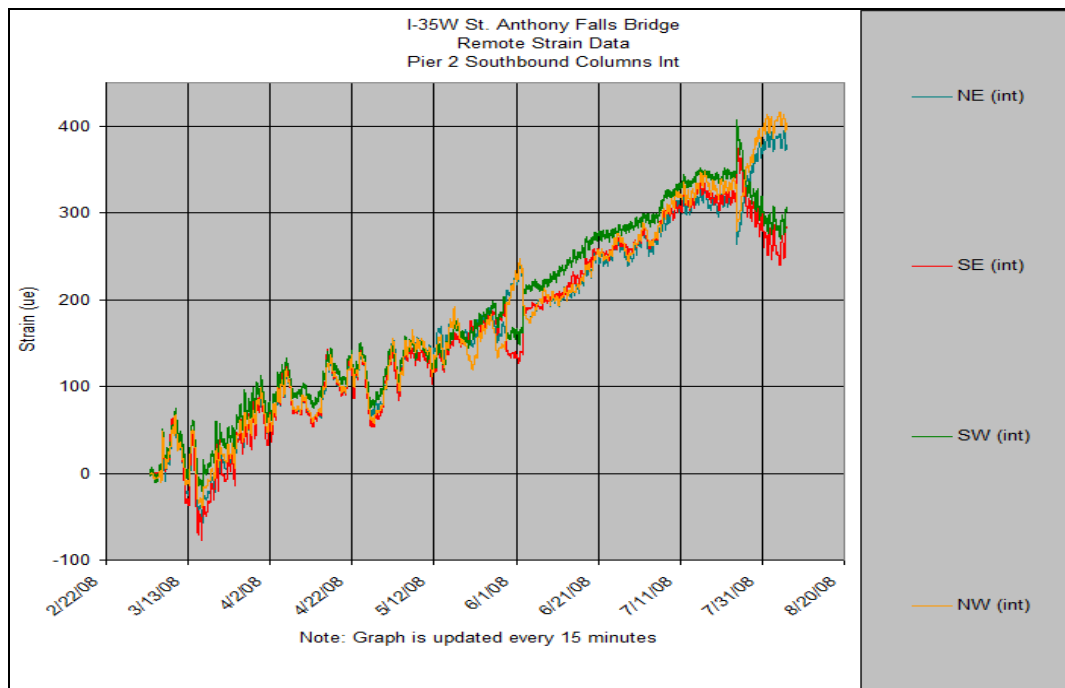

Figure 95. Graph. Strains measured in the interior column of pier 2 southbound.
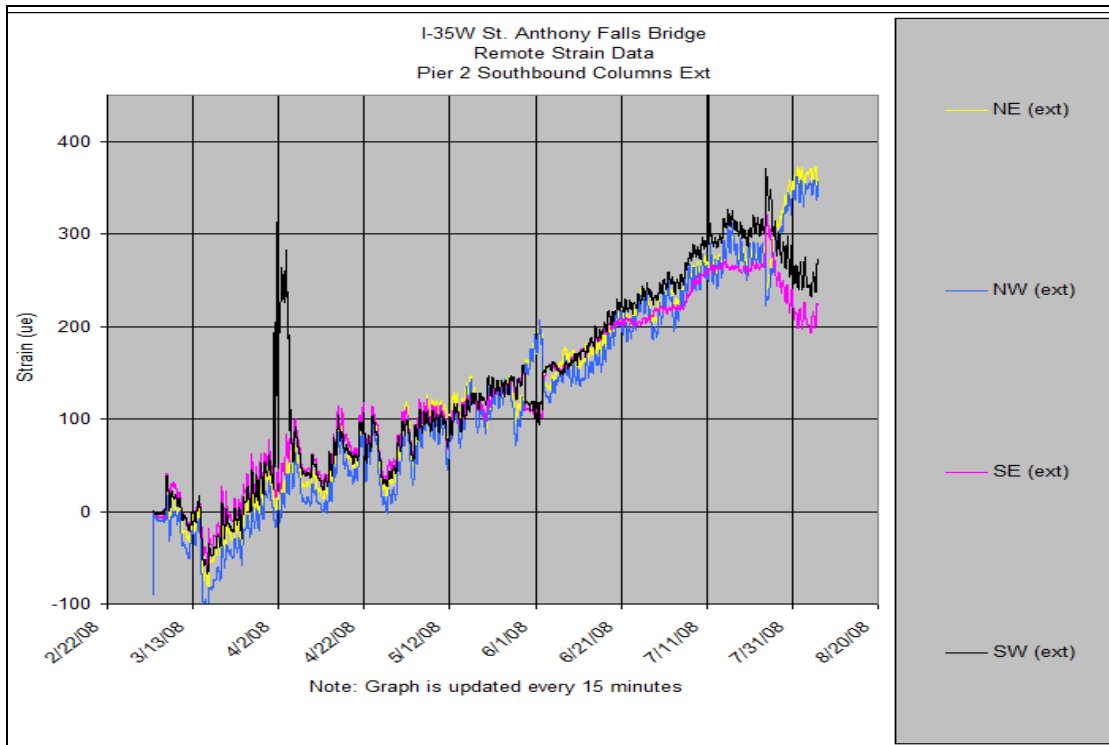
Figure 96. Graph. Strains measured in the exterior column of pier 2 southbound.

Upon further review of these data with the structural engineer, the drastic reduction in strains which resulted in returning to the somewhat normal values was a result of the internal prestressing of the entire section. The ±75–100 μe values shown in the columns were a direct result of a pier movement (away from midspan) of approximately 0.75 inches (19.05 mm) (from field observations). Subsequent prestressing must therefore have resulted in a permanent net movement (toward midspan) of a similar magnitude or approximately 0.75 inches (19.05 mm).

All temporary DAS boxes were again removed to allow the construction of a public viewing platform beneath pier 2 (adjacent to the river). At the time of removal, it was thought that the permanent DAS would be installed within the week in a vault cast aside the northwest corner of the footing (pier 2 southbound). Ultimately, nearly 1 month of data were lost during this disconnection period. Furthermore, it was not clear at that time whether the substructure gauges would be online for the truck tests series scheduled for the following month.

PHASE III—LONG-TERM HEALTH MONITORING

The third and final phase of SSHM for the St. Anthony Falls Bridge Monitoring Project was the long-term health monitoring of the substructure, which was synchronized with the superstructure system. In phase III, the loads induced on the entire bridge by the ongoing daily use of the bridge were monitored as well as those effects caused by diurnal and seasonal temperature variations. The timeline shown in figure 46 indicates that long-term monitoring should have commenced upon completion of the bridge which opened on September 18, 2008, more than 3 months early. However, no live load, diurnal, or seasonal data were available at the time of this report (6 months after the bridge opening), with the exception of several days of monitoring that included live load truck tests.

The long-term monitoring program also included numerous superstructural instrumentation regimes involving deck corrosion, box girder vibrations, box girder strains, etc., which were outside the scope of the SSHM program. SSHM was incorporated into the overall health monitoring of the bridge via an onsite DAS building located east of the north end of the bridge. Therein, various systems were housed to monitor the various gauge types used throughout the bridge. For the SSHM components, two systems are presently being used that replaced the temporary DAS systems described previously. Both systems act as repeaters, whereby the data are collected and transmitted via Ethernet or similar communication to the far end of the bridge (over 1,000 ft (305 m)).

Live Load Truck Tests

Live load testing of the completed bridge using weighed trucks was conducted 4 days prior to the bridge opening. Although the intention was to have data collected from both the substructural and superstructural instrumentation by the permanent DAS, it became clear 2 days prior to the test that the substructure gauges would not be connected to any unit (temporary or permanent). To that end, FGE, LLC sent personnel to the I-35W bridge site the day before the testing to reconnect to the temporary DAS units, assuring this valuable information was not lost.

Figure 97 shows the temporary DAS being reconnected to the southbound pier 2 footing. The vault in which the permanent repeater DAS units are to be housed is formed with plywood just behind the temporary DAS units shown. The units were reconfigured to record at higher rates (one sample/minute for resistive gauges and two samples/minute for the vibration wire gauges). The 2-min sampling rate for the vibrating wire gauges was the limiting (high-end) rate dictated by the number of gauges, the multiplexers, and the basic physics of the gauge type. The faster resistive gauges were recorded at a 1-min logging rate, but the DAS was sampling at 100 Hz. As before, logging of this device incorporated maximum, minimum, average, and instantaneous readings as accumulated over the 1-min logging interval.

Figure 97. Photo. Temporary DAS system reconnected, reconfigured, and reattached in new location adjacent to the permanent DAS subpanel vault.

Truck testing involved eight fully loaded dump trucks (50,000 lb (22,700 kg) each) driven in a series of patterns across the bridge. Starting with a side-by-side configuration (eight abreast), the trucks began at pier 3 (north side of the river) on the southbound structure and moved systematically across to the south, stopping at prescribed locations (e.g., pier 3, quarter points, midpoint, pier 2, etc.). Figure 98 shows one such truck configuration.


Figure 98. Photo. Trucks (400-kip (181,436.95-kg) total load) staged at predetermined location.

One of the many convenient features of the temporary DAS was the wireless/remote reconfiguration options that allowed onsite or in-office access to the system. While onsite during the afternoon before the truck test, both the vibrating wire and resistive gauge systems were reconfigured via cellular internet access to the host computer in Tampa, FL. Although the host was remotely accessed from the field, all data were being logged to the secure site on 5-min intervals.

The first series of truck tests were conducted over a 10-h period beginning at 7 p.m. on September 14, 2008, and concluding at 5 a.m. on September 15, 2008. Figure 99 shows the raw data as updated on the host Web site every 5 min. All strains were zeroed once the DAS units were reconnected, which represented live load measurements and showed minute changes in strain due to the truck loads. Figure 100 through figure 102 show a single load cycle for the columns, shaft 1, and shaft 2, respectively. Given the calibration and understanding of the column strain magnitudes afforded by the closure pour strains (±75–100 µe represented a 0.75-inch (19.05-mm) top of column movement), it is clear that as the trucks approached mid-span at approximately 8:30 p.m., the columns moved outward approximately 0.05–0.07 inches (1.27–1.78 mm). This was caused by a slight loss of camber from the centrally located concentrated load. The steps in the data were congruous to the times in which the trucks were either stopped at a given location (10–15-min holds) or moving to the next location. It can also be seen that multiple load cycles were conducted up until the time at which the contractor took over to complete other aspects of the bridge in the early morning hours of that day. This set of tests was denoted as the static truck tests due to the long holding periods. Figure 101 and figure 102 clearly show live load effects all the way down to the toe of each shaft.
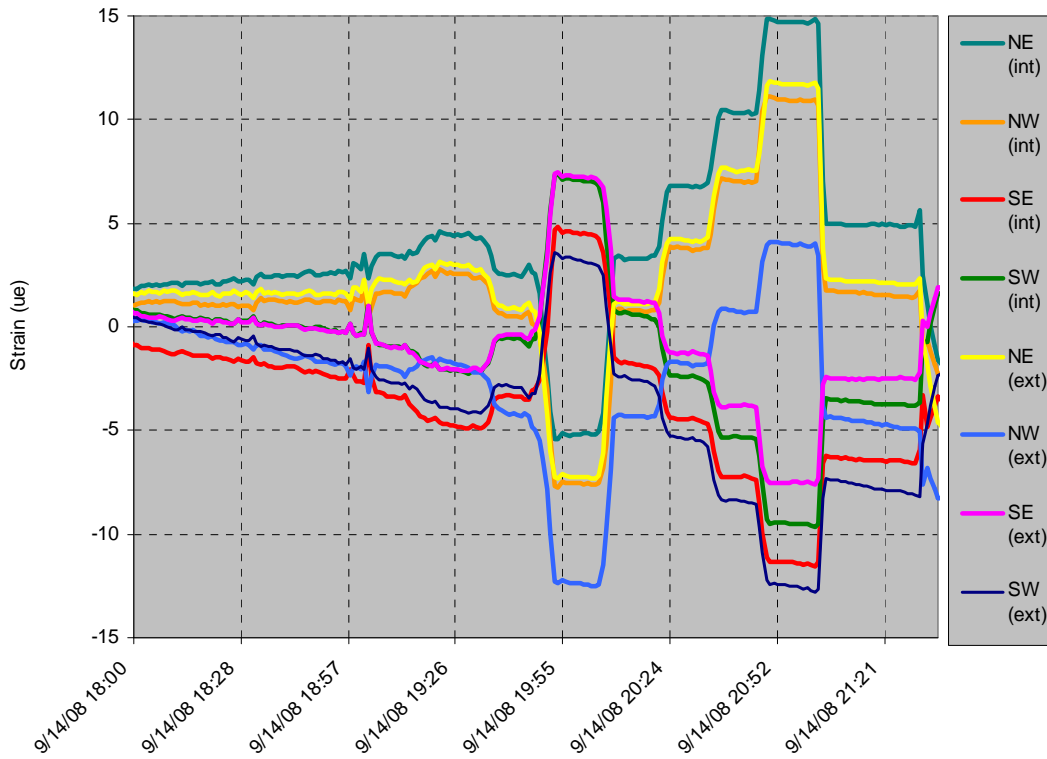
Figure 99. Graph. Column strains during 10-h truck tests (positive compression).

I-35W St. Anthony Falls Bridge Live Load Truck Tests
Remote Strain Data
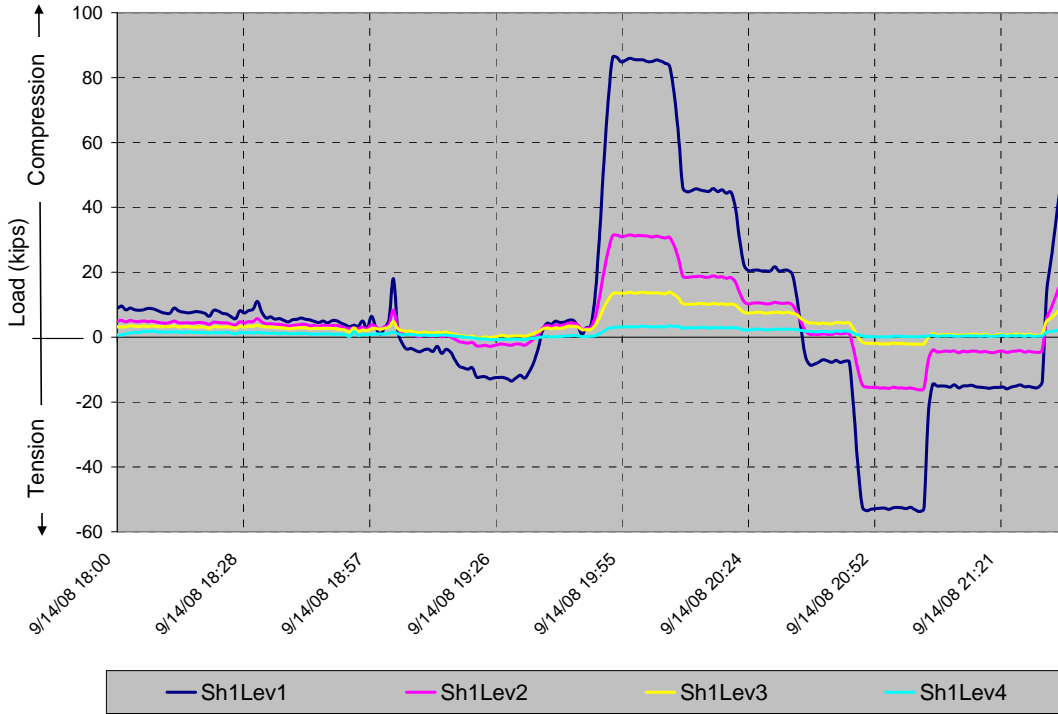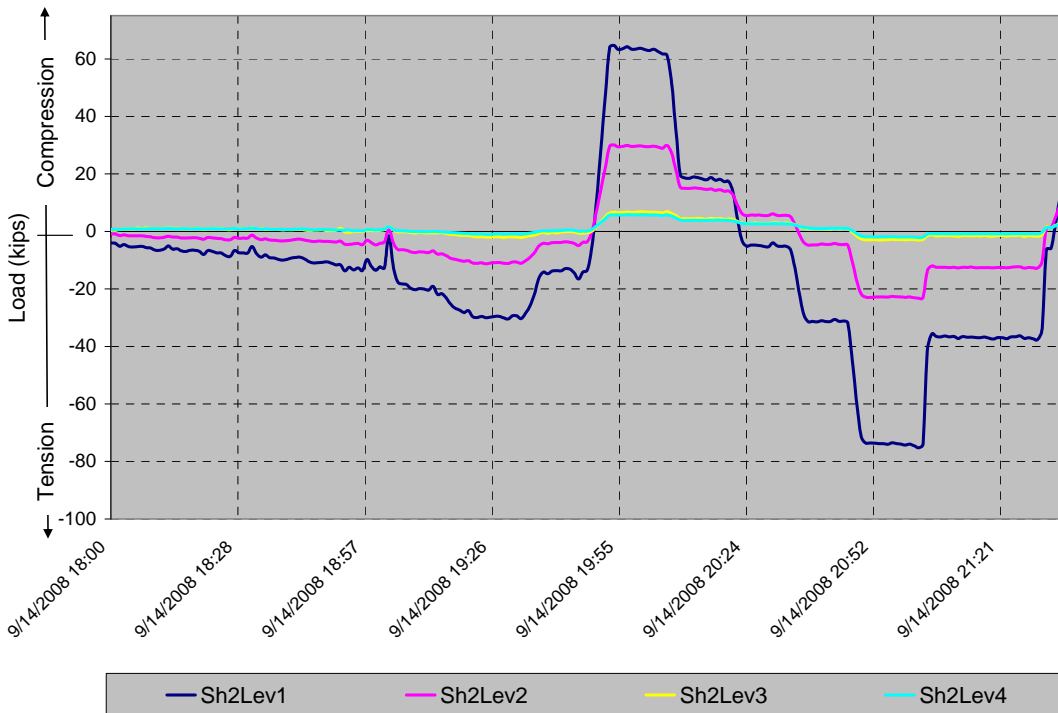Pier 2 Southbound Columns Int and Ext
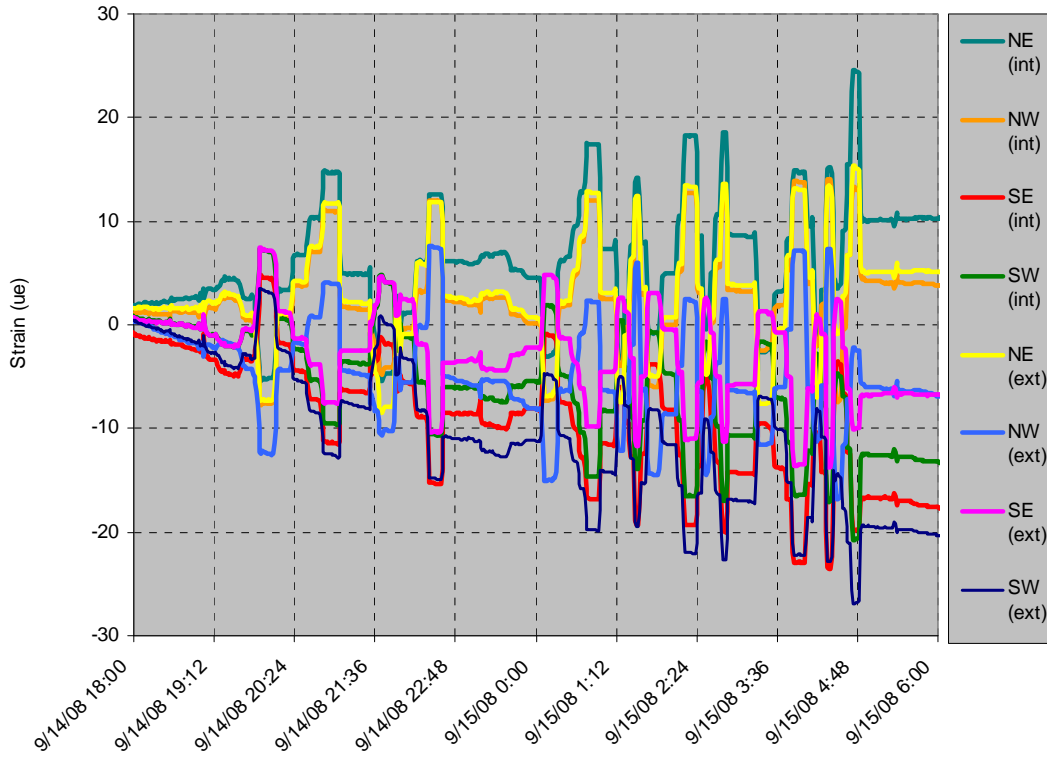
Note: Graph is updated every 5 minutes

Figure 100. Graph. Truck load test results for both columns for one cycle of truck positions.

81

1 kip = 454 kg

Figure 101. Graph. Truck load test results for shaft 1 for one cycle of truck positions.

1 kip = 454 kg

Figure 102. Graph. Truck load test results for shaft 2 for one cycle of truck positions.

82

The temporary DAS was left in place for several days in hopes of capturing data from a series of 45-mi/h (72.45-km/h) dynamic truck loadings scheduled later in the week (but prior to the bridge opening at 5 a.m. on September 18, 2008). Figure 103 through figure 106 show a 4.5-day data window starting with the static truck tests on September 14, 2008, and show the effect of diurnal temperature variations through this period. In each of these graphs, the reported temperature for Minneapolis, MN, over that same timeframe is superimposed and virtually mimics the overall strain trends (with the exception of the truck test strains) for four of the eight column gauges. The other four show an opposite effect. Those gauges on the column face closest to the main span (north side) and should experience tension with increased temperature of the main span girders due to thermal expansion. Shaft loads increased as the bridge warmed and expanded, thereby pushing down on the south edge of the footing, which corresponds to the locations of shafts 1 and 2.
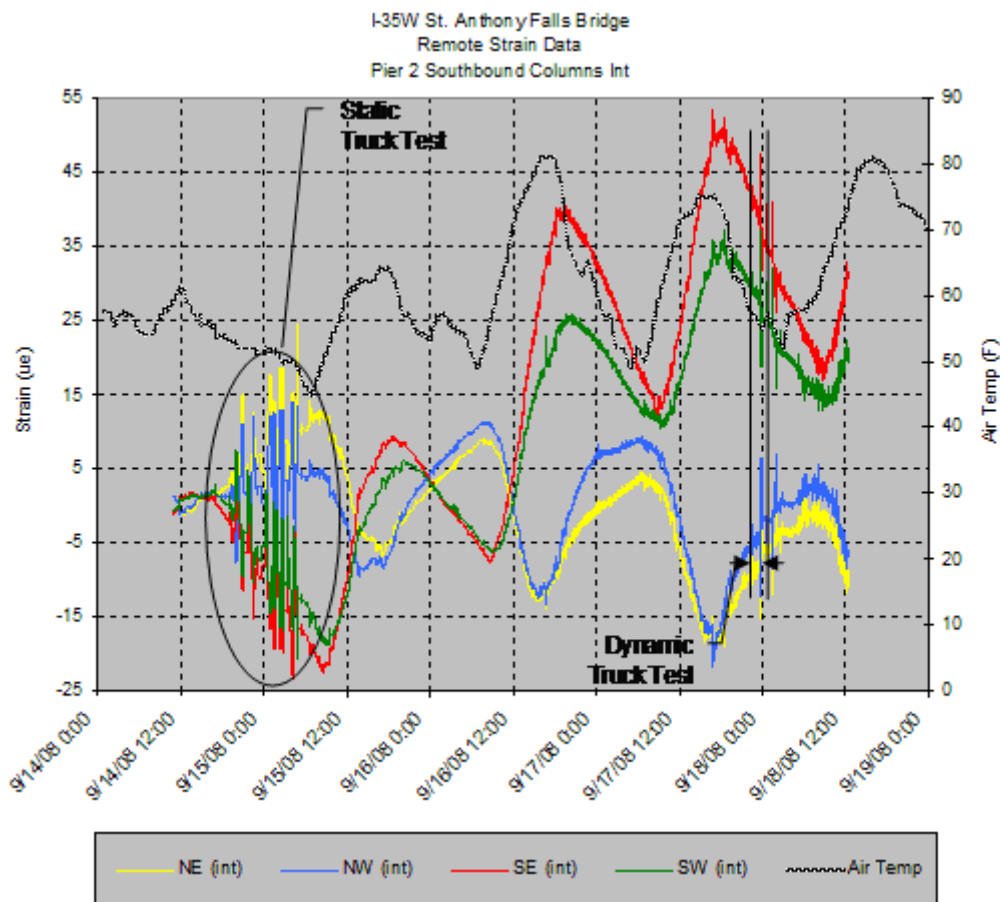

Figure 103. Graph. Live load effects on the interior column over 4.5-day period.
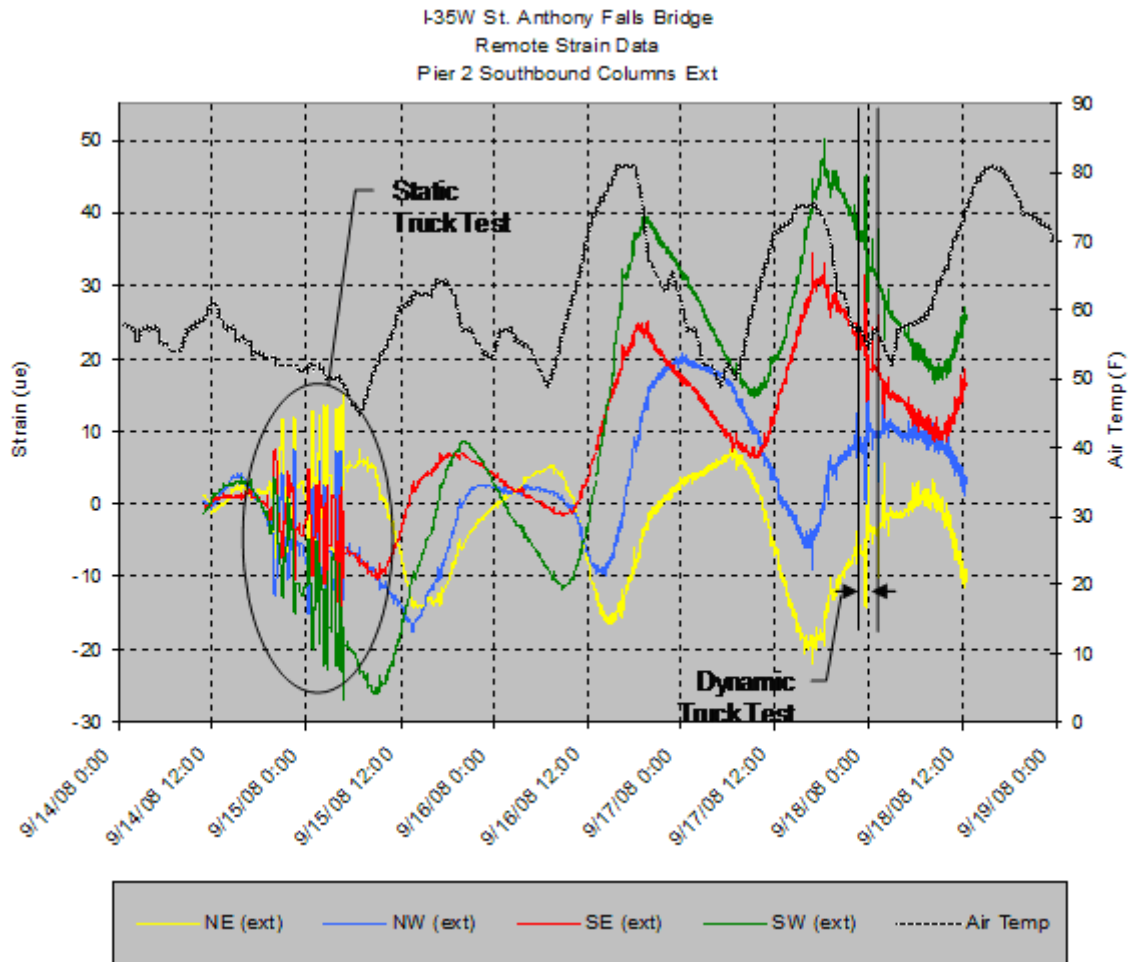
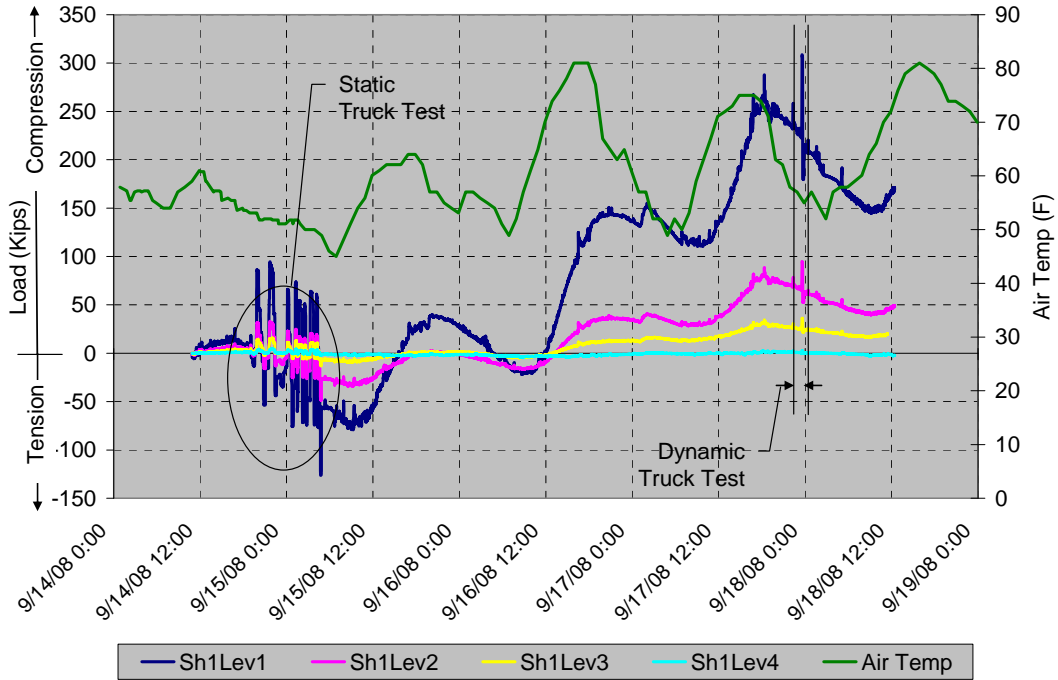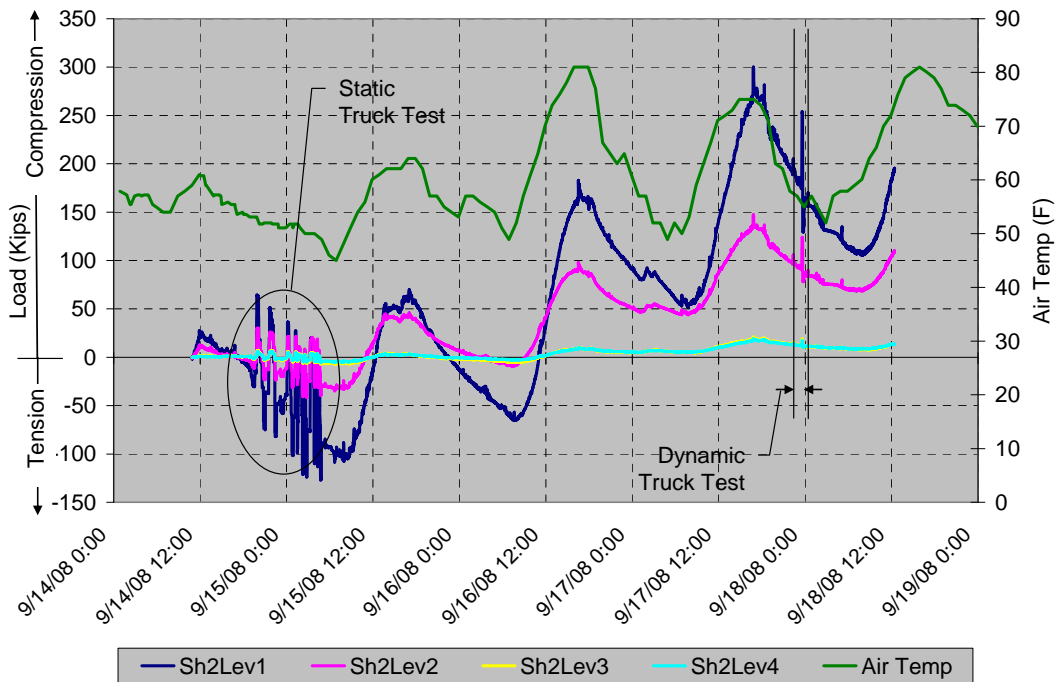**Figure 104. Graph. Live load effects on the exterior column over 4.5-day period.**

1 kip = 454 kg
°F = 1.8(°C) + 32

Figure 105. Graph. Live load effects on shaft 1 over 4.5-day period.

1 kip = 454 kg
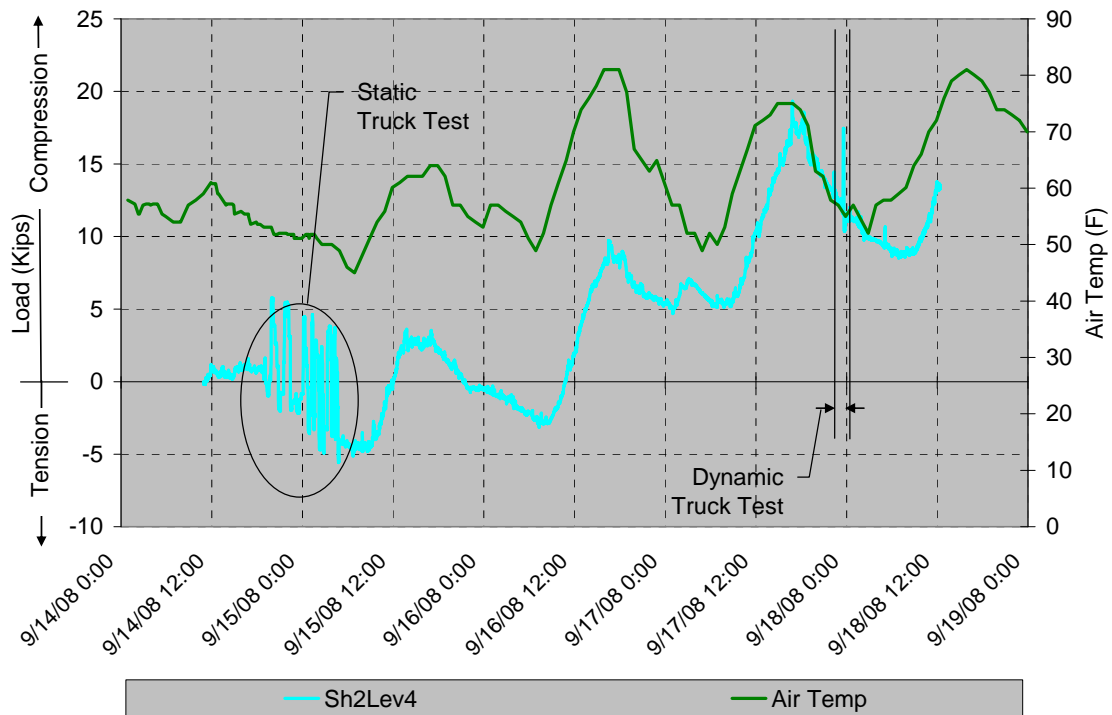°F = 1.8(°C) + 32

Figure 106. Graph. Live load effects on shaft 2 over 4.5-day period.

85

As subsequent dynamic truck tests were scheduled for later that week, the temporary DAS units were left in place in hopes of obtaining the data or until the last possible moment after which the wooded forms to which the units were attached needed to be stripped (see figure 97). Although details of the exact loading event were not available at the time of reporting, the effects of the events were captured, as indicated in figure 103 through figure 106.

System Results and Conclusions

In the absence of long-term monitoring data for the last 6 months, it was difficult to demonstrate the full benefit of the system as it is presently equipped. However, from the small window of available information shown in figure 99 through figure 107, it is clear that the equipment has tremendous capability to detect subtle loading throughout the substructure. Figure 107 shows a scale-enhanced version of figure 106 wherein the moderate daily temperature fluctuations of 20 °F (-6.67 °C) induced axial load variations of approximately 10 kips (4,535.92 kg) at the toe of shafts. Interestingly, the Minneapolis, MN, area can see annual temperature fluctuations of over 100 °F (37.78 °C), which should be easily captured with the SSHM system. Furthermore, the data show live load effects caused by truck loading with magnitudes as much as 5 kips (2,270 kg). It should be noted that these effects are caused by lever arm effects from forces acting horizontally at the top of the column. These are the exact types of forces that typically control foundation design.

1 kip = 454 kg
°F = 1.8(°C) + 32

Figure 107. Graph. Diurnal temperature and truck load effects at the toe of shaft 2.

Finally, the results of the truck load tests (although incomplete at the time of this report) served to calibrate the column strain measurements over the entire cross section by taking the sum of the individual average column strains and applying a known concrete modulus. Figure 108 shows the force computed from strain, column cross sectional area, and modulus during the truck load tests where the 400-kip (181,600-kg) total truck loads are corroborated. This also shows that as the trucks were loaded directly over pier 2 (the SSHM project site), some torsion of the box girders and deck assembly caused a slight uplift on the exterior column as trucks were lined up starting from the opposite interior column (east) side of the deck. A similar increased load was observed on the interior column corresponding to the cantilevered loading from that edge of the deck.
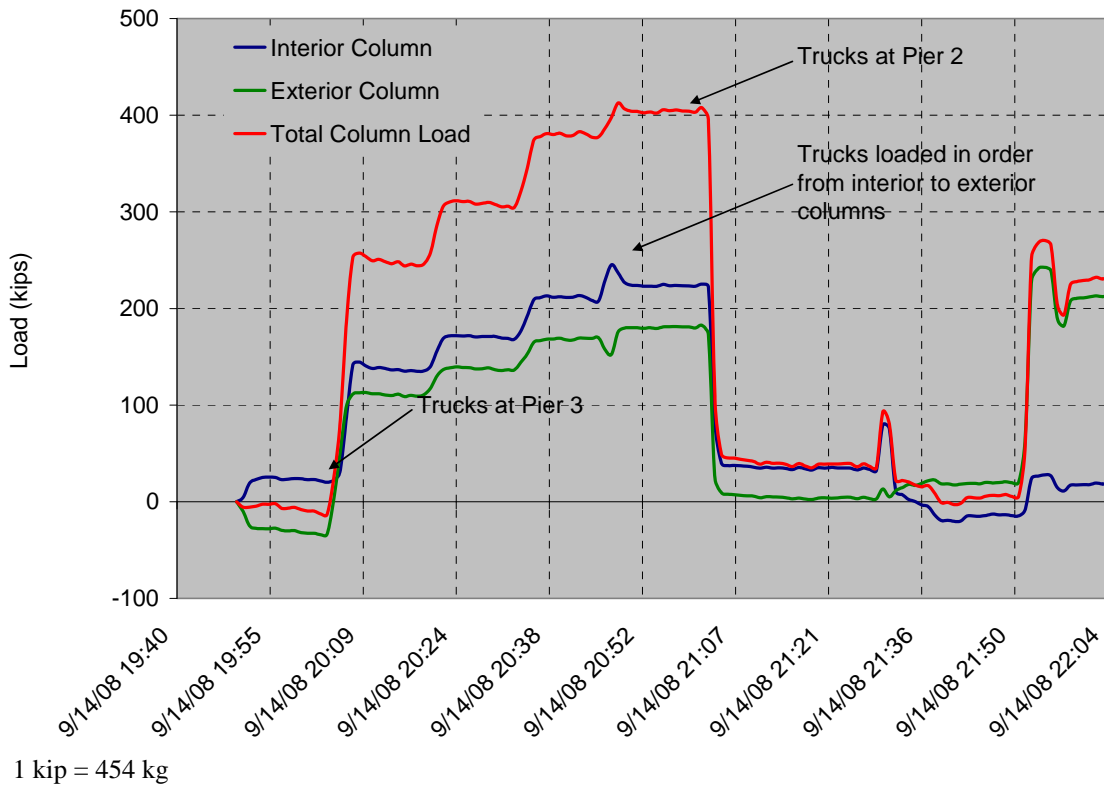

1 kip = 454 kg

Figure 108. Graph. Column gauge calibration from known truck loads.

CHAPTER 5. SUMMARY AND CONCLUSIONS

This project was originally intended to show the merits of SSHM via a review of the few well-documented cases where a concerted effort was in place to assess the long-term performance of foundations. While these efforts were underway, the I-35W bridge over the Mississippi River in Minneapolis, MN, collapsed in the middle of rush hour, killing 13 people and revealing to engineers the United States' failing infrastructure. As a result, the project was redirected to aid MnDOT and FHWA in providing an effective yet economical means to monitor the new substructure during construction and for the future. This was possible largely due to the preparedness afforded to the research team as a result of the ongoing study. Therein, DAS units being tested on other sites could be redeployed immediately to obtain data for this fast-paced design-build bridge replacement project.

Two sites served as the primary proving grounds for the study: (1) the voided shaft test site in Clearwater, FL, and (2) the bridge replacement site in Minneapolis, MN. In both cases, data were obtained from below the ground surface from embedded instrumentation and used both to assess the health and performance of the elements and to review the capabilities of low-cost DAS. In that regard, hundreds of vendors provided DAS units of varied performance and economy, but this study chose to assess companies' units to a large degree based on the cost. The ability to obtain data, upload remotely to a host server, and make spontaneous changes to the system configuration without a site visit were explored to the fullest. With very few exceptions, the systems performed well with an approximate cost of $160 per channel sampled for site 1 (Florida) and $170 per channel for site 2 (Minnesota). These prices included the loggers, cellular modems, enclosures, and power supply systems but did not include the cellular service contracts which were generally annual or biannual agreements. Embedded instrumentation varied and was generally more for site 2 based on the type of sensor.

A large amount of data was collected from site 2 and conceivably continues to be gathered (although presently unknown at the time of reporting). These data can be found in the attached appendix for completeness (archival purposes). Due to its electronic nature, it is readily usable for future analyses. Much of the analysis of these data is presented in chapter 4, but there are unanswered performance questions that remain. A full year of data collection is recommended to assess the substructure performance at the very minimum. This is presumably the course of action presently underway by MnDOT. However, multiple years and extreme weather events are likely to prevail that need to be caught by the DAS and used to alert transportation officials of possible changes in the substructural conditions.

REFERENCES

1. Clark, R. and Feldman, A. (2002). *Continued Monitoring of Pier EA-31, West Seattle Freeway Bridge, Seattle, Washington*, Order No. DTFH61-02-P-00197, Seattle, WA.

2. Arms, S., Galbreath, J., Newhard, A., and Townsend, C. (2004). *Remotely Programmable Sensors for Structural Health Monitoring*, Structural Materials Technology (SMT): NDE/NDT for Highways and Bridges, Buffalo, NY.

3. Susoy, M., Zaurin, R., and Catbas, F. (2006). *Development of a Structural Health Monitoring Framework for the Movable Bridges in Florida*, Submitted for Transportation and Research Board's 86th Meeting, Washington, DC.

4. Watters, D., Jayaweera, P., Bahr, A., and Huestis, D. (2001). *Design and Performance of Wireless Sensors for Structural Health Monitoring,* SRI International, Menlo Park, CA.

5. Udd, E., Schulz, W., Seim, J., Laylor, M., Soltesz, S., and Inaudi, D. (2000). *Single and Multi-Axis Fiber Grating Strain Sensor Systems for Bridge Monitoring*, Conference on Trends in Optical Non-Destructive Testing, Lugano, Switzerland.

6. Hemphill, D. (2004). *Structural Health Monitoring System for the East 12th Street Bridge*, Iowa State University, Ames, IA.

7. Weyl, L. (2005). *Developing a Web-Based Management System for the Indian River Inlet Monitoring Plan*, Research Experiences for Undergraduates in Bridge Engineering, University of Delaware, Newark, DE.

8. Google Maps. (2008). *Map of voided shaft testing site*. Data date: 2008, Generated by: Gray Mullins via Google Maps online, obtained from: http://maps.google.com/. Generated June 5, 2008.

9. Minnesota Department of Transportation. *I-35W St. Anthony Falls Bridge*, St. Paul, MN. Obtained from: http://projects.dot.state.mn.us/35wbridge/index.html.